

Longitudinal study of DNA methylation and epigenetic clocks prior to and following test-confirmed COVID-19 and mRNA vaccination

1 Alina PS Pang^{1#}, Albert T. Higgins-Chen^{2,3#}, Florence Comite^{4,5}, Ioana Raica⁴, Christopher
2 Arboleda⁴, Hannah Went⁶, Tavis Mendez⁶, Michael Schotsaert^{7,8}, Varun Dwaraka⁶, Ryan
3 Smith⁶, Morgan E. Levine⁹, Lishomwa C. Ndhlovu¹, Michael J. Corley^{1*}

4 ¹ Division of Infectious Diseases, Department of Medicine, Weill Cornell Medicine, New York, NY,
5 USA

6 ²Department of Psychiatry, Yale University School of Medicine, New Haven, CT, USA

7 ³VA Connecticut Healthcare System, West Haven, CT, USA

8 ⁴Comite Center for Precision Medicine & Health, New York, NY, USA

9 ⁵Lenox Hill Hospital/Northwell, New York, NY, USA

10 ⁶TruDiagnostic, Lexington, KY, USA

11 ⁷Department of Microbiology, Icahn School of Medicine at Mount Sinai, New York, NY, USA

12 ⁸Global Health and Emerging Pathogens Institute, Icahn School of Medicine at Mount Sinai, New
13 York, NY, USA

14 ⁹Department of Pathology, Yale University School of Medicine, New Haven, CT, USA

15

16 **#Authors Contributed Equally**

17 *** Correspondence:**

18 Corresponding Author

19 Michael J. Corley, MA, PhD, Assistant Professor, Department of Medicine, Division of Infectious
20 Diseases, Weill Cornell Medicine, 413 East 69th St., New York, NY 10021 Email:

21 mjc4002@med.cornell.edu

22

23

24

25

26

27 **Keywords: COVID-19, DNA methylation, epigenetics, aging, epigenetic clock**

28

29 **Abstract**

30 The host epigenetic landscape is rapidly changed during SARS-CoV-2 infection and evidence suggests
31 that severe COVID-19 is associated with durable scars to the epigenome. Specifically, aberrant DNA
32 methylation changes in immune cells and alterations to epigenetic clocks in blood relate to severe
33 COVID-19. However, a longitudinal assessment of DNA methylation states and epigenetic clocks in
34 blood from healthy individuals prior to and following test-confirmed non-hospitalized COVID-19 has
35 not been performed. Moreover, the impact of mRNA COVID-19 vaccines upon the host epigenome
36 remains understudied. Here, we first examined DNA methylation states in blood of 21 participants
37 prior to and following test confirmed COVID-19 diagnosis at a median timeframe of 8.35 weeks. 261
38 CpGs were identified as differentially methylated following COVID-19 diagnosis in blood at an FDR
39 adjusted P value <0.05 . These CpGs were enriched in gene body and northern and southern shelf
40 regions of genes involved in metabolic pathways. Integrative analysis revealed overlap among genes
41 identified in transcriptional SARS-CoV-2 infection datasets. Principal component-based epigenetic
42 clock estimates of PhenoAge and GrimAge significantly increased in people over 50 following
43 infection by an average of 2.1 and 0.84 years. In contrast, PCPhenoAge significantly decreased in
44 people under 50 following infection by an average of 2.06 years. This observed divergence in
45 epigenetic clocks following COVID-19 was related to age and immune cell-type compositional
46 changes in CD4⁺ T cells, B cells, granulocytes, plasmablasts, exhausted T cells, and naïve T cells.
47 Complementary longitudinal epigenetic clock analyses of 36 participants prior to and following Pfizer
48 and Moderna mRNA-based COVID-19 vaccination revealed vaccination significantly reduced
49 principal component-based Horvath epigenetic clock estimates in people over 50 by an average of 3.91
50 years for those that received Moderna. This reduction in epigenetic clock estimates was significantly
51 related to chronological age and immune cell-type compositional changes in B cells and plasmablasts
52 pre- and post-vaccination. These findings suggest the potential utility of epigenetic clocks as a
53 biomarker of COVID-19 vaccine responses. Future research will need to unravel the significance and
54 durability of short-term changes in epigenetic age related to COVID-19 exposure and mRNA
55 vaccination.

56

57

58

59

60

61 **1 Introduction**

62 Epigenetic mechanisms including DNA methylation are critically involved in both host
63 immune responses to viral infection and subsequent diseases pathogenesis and severity (Gómez-Díaz
64 et al., 2012; Morales-Nebreda et al., 2019). In the context of SARS-CoV-2 infection, human studies
65 suggest that DNA methylation states in immune cells are altered during infection and associate with
66 COVID-19 disease severity (Bernardes et al., 2020; Balnis et al., 2021; Castro de Moura et al., 2021;
67 Corley et al., 2021). We previously reported a unique candidate immune cell DNA methylation
68 signature associated with severe COVID-19 that was distinct from influenza, primary HIV infection,
69 and HIV/mild COVID-19 coinfection (Corley et al., 2021). Additional studies have extended these
70 findings and reported distinct genome-wide DNA methylation differences in peripheral blood from
71 COVID-19 patients based on disease severity (Balnis et al., 2021; Castro de Moura et al., 2021; Zhou
72 et al., 2021). Insights into host DNA methylation states and COVID-19 have mainly focused on
73 severe COVID-19 and are limited by the use of cross-sectional study designs. Longitudinal
74 epigenetic studies of COVID-19 are lacking, and it remains unclear whether rapid changes to
75 immune cell epigenetic DNA methylation patterns occur in healthy individuals that recover from
76 non-hospitalized COVID-19.

77 The severity of COVID-19 strongly depends on age, and aging biomarkers may help explain
78 this relationship and predict who is at highest risk of severe COVID-19 (Kuo et al., 2020; Mueller et
79 al., 2020). Distinct DNA methylation patterns have been utilized to derive epigenetic measures of
80 biological aging termed “epigenetic clocks”(Horvath, 2013). Numerous epigenetic clocks have been
81 generated that appear to capture distinct aspects of aging and associate with different biological
82 hallmarks of aging, environmental exposures, traits, and disease patterns (Horvath and Raj, 2018; Liu
83 et al., 2020; Higgins-Chen et al., 2021a; Oblak et al., 2021). Many of the differences between clocks

84 stem from being trained to predict different aging-related variables, such as chronological age,
85 mortality risk, or mitotic divisions. Moreover, epigenetic clocks are accurate predictors of mortality
86 risk (Lu et al., 2019), biomarkers of pathogen exposure (Horvath and Levine, 2015; Boulias et al.,
87 2016; Corley et al., 2021), and correlates of lung function and immune inflammation (Hillary et al.,
88 2020, 2021). Evidence suggests that severe COVID-19 disease may impact certain epigenetic clocks
89 (Corley et al., 2021; Mongelli et al., 2021a) and biological aging captured by PhenoAge may inform
90 COVID-19 outcomes (Kuo et al., 2020). More recent epigenetic clock studies have reported
91 conflicting evidence for biological age acceleration and telomere shortening in COVID-19 survivors
92 (Mongelli et al., 2021b), with some finding no clock acceleration in COVID-19 patients (Franzen et
93 al., 2021). Whether changes occur to epigenetic clocks in healthy individuals that recover from non-
94 hospitalized COVID-19 remains unclear. Additionally, whether epigenetic clocks are impacted
95 following mRNA COVID-19 vaccination remains understudied.

96 In this study, we first examined whether alterations to DNA methylation states, blood immune
97 cell type composition, and epigenetic clocks occurred in peripheral blood following COVID-19 using
98 a longitudinal study design of 21 healthy participants prior to and following test-confirmed COVID-
99 19. Next, we also evaluated longitudinal DNA methylation states, blood immune cell type
100 composition, and epigenetic clocks of 36 healthy participants prior to and following complete two-
101 dose mRNA-based COVID-19 vaccination.

102

103 **2 Results**

104 **2.1 Cohort of participants with longitudinal assessments of DNA methylation prior to and** 105 **following test-confirmed COVID-19 infection.**

106 **Table 1** presents the baseline (pre-COVID-19) characteristics of study participants prior to
107 COVID-19 diagnosis. Participants were healthy (n=14M, 7F) and ranged in chronological age from
108 18 to 73 years (Median = 46 years). Genome-wide DNA methylation was assayed from blood
109 biospecimens of all participants at baseline and post-COVID-19 using the Illumina MethylationEPIC
110 platform (Pidsley et al., 2016). Baseline DNA methylation for participants was obtained at a median
111 of 19 weeks prior to the first COVID-19-positive test (Range: 4 - 50 weeks). COVID-19 exposure
112 and SARS-CoV-2 infection of participants for the post-COVID-19 timepoint was confirmed utilizing
113 clinical PCR testing (n=18) and serology testing (n=3). Post-COVID-19 DNA methylation was
114 assessed at a median timeframe of 8.35 weeks after testing positive. The earliest captured
115 participant's post-COVID-19 DNA methylation was within 1 week following COVID-19 diagnosis
116 and ranged out to a maximum of 6 months after diagnosis.

117 **2.2 Differentially methylated loci following SARS-CoV-2 infection.**

118 To identify differentially methylated loci in blood related to COVID-19, we utilized a
119 longitudinal study design that included genome-wide DNA methylation data generated from 21
120 participants prior to (pre-COVID-19) and following COVID-19 diagnosis (post-COVID-19)
121 (**Fig.1a**). Our repeated measures analysis of DNA methylation at pre- and post-COVID-19 timepoints
122 revealed 756 differentially methylated loci significant at FDR (Benjamini-Hochberg) adjusted $P <$
123 0.05 that were not significantly biased to a specific chromosomal location (**Fig.1b, Supplementary**
124 **Dataset 1**). 57.8% of the COVID-19 related DML were increases in DNA methylation states (hyper-
125 methylation) at the post-COVID-19 compared to pre- timepoint for participants. Next, we examined
126 whether these COVID-19 related DML in blood were enriched in specific genomic contexts and
127 found a significant enrichment in gene body (Odds Ratio= 1.2 ; $P = 0.005$) and northern (Odds
128 Ratio= 1.7 ; $P = 0.0004$) and southern (Odds Ratio= 1.8 ; $P = 0.0001$) shelf regions located adjacent
129 to CpG island shore regions compared to the expected distribution of methylation sites assayed

130 across the human genome (**Fig.1c**), suggestive of perturbations at regulatory regions in the human
131 genome likely linked to transcriptional differences. We observed that the 756 COVID-19 associated
132 DML were related to 516 annotated protein coding genes (**Supplementary Dataset 1**). Gene
133 enrichment analysis revealed the top biological processes involved cellular glucose homeostasis (GO:
134 0001678; $P = 0.001$) **Supplementary Figure S1**. KEGG pathway analyses showed the top pathway
135 involved thyroid hormone signaling ($P = 0.00001$) **Supplementary Figure S1**. These findings
136 support the interplay between host metabolism and metabolic gene pathways in COVID-19 and
137 reports of dysregulated glycemia in COVID-19 (Reiterer et al., 2021).

138 Since our assessments of DNA methylation in participants occurred in whole blood, we next
139 applied a bioinformatic tool to identify the potential cellular source in blood of the COVID-19
140 exposure-related differences in participants. We analyzed whether there was an enrichment for
141 overlap with potential functional elements in our set of 756 DML related to COVID-19 compared to
142 matched background DML using the experimentally-derived Functional element Overlap analysis of
143 ReGions from EWAS tool (eFORGE) (Breeze et al., 2019). eFORGE uses 815 datasets from the
144 ENCODE, Roadmap Epigenomics, and BLUEPRINT epigenomic mapping projects to detect
145 enriched tissues, cell types, and genomic regions of DML from DNA methylation profiling studies.
146 Our analysis utilizing the chromatin all 15-state marks reference revealed the greatest enrichment in
147 actively transcribed genes of primary B cells (q value = $3.65e-10$), mononuclear cells (q value =
148 $4.39e-8$), and neutrophils (q value = $1.03e-11$) from peripheral blood suggesting potential cell
149 composition and/or cell type-specific effects of COVID-19 infection in blood (**Supplementary**
150 **Dataset 2**). In addition to these immune cell-type findings, we evaluated whether the observed
151 epigenetic signature mimic methylation changes in SARS-CoV-2 target tissues. This analysis
152 revealed significant enrichment in multiple organ systems supporting COVID-19 as a complex
153 multisystem disorder (**Supplementary Dataset 2**). Notable enrichments were observed in actively

154 transcribed genes of the digestive system (sigmoid colon, q value = 8.42e-8; duodenum smooth
155 muscle, q value = 5.06e-8; rectal mucosa, q value = 3.19e-7; duodenum mucosa, q value = 3.19e-7),
156 placenta (q value = 6.21e-06), spleen (q value = 1.25e-05, brain (anterior caudate, q value= 1.32e-05;
157 hippocampus, q value= 2.13e-05), liver (q value = 3.92e-05), and lung (q value = 9.22e-05)
158 **(Supplementary Dataset 2)**. These data support the notion of COVID-19 impacting the epigenetic
159 landscape as a multisystem disorder involving both immune cells and nonimmune cells in disease
160 pathogenesis.

161 Among the top $\Delta\beta$ -value methylation changes comparing pre- and post-COVID-19 timepoints,
162 we observed two differentially methylated loci (cg02037503 and cg23712970) in a gene promoter
163 transcription start site regulatory region of the apoptotic chromatin condensation inducer 1 (*ACINI*)
164 gene **Supplementary Figure S2** that decreased in DNA methylation following COVID-19 by
165 approximately 15% for both CpG sites (**Fig.1d,e**). This gene codes a nuclear protein that induces
166 apoptotic chromatin condensation after activation by caspase-3 (Sahara et al., 1999), which we
167 previously reported was increased in red blood cells of hospitalized COVID-19 participants
168 (Plassmeyer et al., 2021). We also observed differential methylation at cg10846936 related to the
169 caspase recruitment domain family member 14 (*CARD14*) gene that is involved in activating nuclear
170 factor-kappa-B involved in immune inflammation. Participants' methylation levels at this loci
171 increased comparing pre- and post-COVID-19 timepoints from a mean of 44.47% to 53.44% (**Fig.1f**).
172 Using a validation analysis of this loci in a public COVID-19 DNA methylation dataset GSE168739
173 (Castro de Moura et al., 2021), we observed that the mean methylation state of this loci in participants
174 post-COVID-19 timepoint (mean DNAm = 53.5%) was more similar ($P = 0.15$, Tukey's test) than
175 participants pre-COVID-19 levels (mean DNAm = 44.6%) ($P = 0.0001$, Tukey's test) compared to
176 levels of this loci in a public blood DNA methylation dataset available from 407 confirmed COVID-
177 19 participants (mean DNAm = 56.5%) (Castro de Moura et al., 2021) **Supplementary Figure S3**.

178 Additional top differentially methylated loci related to the corticotropin releasing hormone receptor 1
179 (*CRHR1*, cg09422970; **Fig.1g**), HIVEP Zinc Finger 3 (*HIVEP3*, cg11857452; **Fig.1h**), Meis
180 Homeobox 2 (*MEIS2*, cg06471042; **Fig.1i**), Nuclear Receptor Coactivator 2 (*NCOA2*, cg20282780;
181 **Fig.1j**), Progesterone Immunomodulatory Binding Factor 1 (*PIBF1*, cg00531853 and 15128396;
182 **Fig.1k,l**), and Sterile Alpha Motif Domain Containing 4A (*SAMD4A*, cg18499294; **Fig.1m**) genes.

183

184 **2.3 DNA methylation-based estimates of cell-type fractions in blood are significantly changed** 185 **following COVID-19 infection.**

186 DNA methylation data can be utilized to infer fractions of immune cell types present in a
187 heterogenous blood sample based on a reference list of CpGs identified from differentially
188 methylated cell-types (Houseman et al., 2012). Hence, we used a paired t-test analysis and examined
189 whether participants DNAm-based estimates of CD8+ T cells, CD4+ T cells, natural killer (NK)
190 cells, B cells, monocytes, granulocytes, plasmablasts, exhausted T cells (CD8+CD28-CD45RA-),
191 CD8 Naïve T cells and CD4 Naïve T cells significantly differed comparing pre- and post-COVID-19
192 timepoints. Since the human immune system undergoes dramatic aging-related changes, we stratified
193 our analysis into two groups based on those under or over 50 years of age. We observed no
194 significant differences in the inferred proportion of CD8+ T cells following COVID-19 for those
195 under and over 50 years of age (**Fig.2a**). Participants under 50 years of age showed significant
196 increases in the percentage of CD4+ T cells in blood following COVID-19 (**Fig.2b**). In contrast, in
197 those over 50 years of age we observed a significant decrease in the percentage of CD4+ T cells in
198 blood following COVID-19 (**Fig.2b**), reflecting COVID-19 reports of lymphopenia. Additionally, we
199 observed significant decreases in the percentage of B cells in those over 50 years of age (**Fig.2d**). In
200 contrast, we observed shifts in decreasing plasmablasts percentage (**Fig.2g**) and increasing CD4+

201 Naïve T cells were observed in those under 50 years of age following COVID-19 (**Fig.2j**). Innate
202 immune NK and monocytes cell proportions did not significantly change following COVID-19
203 (**Fig.2c,e**). We also did not observe significant differences in granulocytes, exhausted CD8+ T cells,
204 and CD8+ naïve T cells (**Fig.2f,h,i**). Together, these findings suggest age-related COVID-19 shifts in
205 specific immune cell types occur in healthy individuals.

206 We utilized the inferred cell type proportional changes following COVID-19 to examine
207 relationships with age and the DNA methylation change pre- vs post-COVID-19 for ten of the top
208 differentially methylated loci we had identified. This correlative analysis showed that chronological
209 age was significantly associated with the percent change in DNA methylation for 9/10 DML,
210 suggesting the signal of change for those DNA methylation sites related to age and potential
211 plasticity loss (**Fig.3**). Moreover, chronological age was significantly associated with the inferred cell
212 type proportional changes following COVID-19 for CD4+ T cells, plasmablasts, and CD4+ naïve T
213 cells adding further support to our observed age-related COVID-19 shifts in specific immune cell
214 types observations (**Fig.3**). Notably, we observed that shifts in inferred immune cell type proportions
215 following COVID-19 significantly related to the extent of DNA methylation level changes for all of
216 the DML we examined suggesting the COVID-19 DNA methylation signature to be substantially
217 influenced by cell-type shifts (**Fig.3**).

218 **2.4 DNA methylation changes in blood following COVID-19 overlap with COVID-19 related** 219 **transcriptional gene sets**

220 Various studies have identified transcriptional changes from SARS-CoV-2 infection(Blanco-
221 Melo et al., 2020; Wilk et al., 2020). Since aberrant DNA methylation is commonly linked to
222 transcriptional alterations, we sought to test whether the 516 genes containing a differentially
223 methylated loci we identified through DNA methylation profiling of pre- and post-COVID-19

224 infection overlapped with COVID-19-related genes transcriptionally altered during SARS-CoV-2
225 infection utilizing the Enrichr COVID-19 gene set online tool (Kuleshov et al., 2016). This analysis
226 revealed significant overlap with genes differentially expressed in SARS-CoV-2 animal models
227 (Rhesus macaques blood, $P = 0.017$; mouse heart, $P = 0.018$; mouse spleen, $P = 0.027$; and hamster
228 blood, $P = 0.027$), COVID-19 human biospecimens (late stage infection blood, $P = 0.027$; human
229 cornea, $P = 0.032$), and *in vitro* infection models (Calu3, $P = 0.030$) (**Table 2**). These findings
230 suggest DNA methylation patterns associated with COVID-19 likely play a role in transcriptional
231 activation or repression of conserved host transcriptional responses to SARS-CoV-2 infection
232 involving specific gene networks.

233 **2.5 Divergence in epigenetic clock estimates based on age related to COVID-19**

234 Previous studies including our work reported epigenetic age perturbations associated with severe
235 hospitalized COVID-19 in older individuals (Corley et al., 2021; Mongelli et al., 2021b). We sought
236 to investigate in this pre- and post-COVID-19 cohort of non-hospitalized COVID-19 and relatively
237 healthy individuals whether COVID-19 exposure impacted epigenetic clock estimates. We calculated
238 epigenetic estimates for Horvath's multi-tissue predictor DNAmAge based on 353 CpG sites (Horvath,
239 2013), the Horvath skin-and-blood clock based on 391 CpG sites (Horvath et al., 2018), Levine
240 DNAmPhenoAge based on 513 CpG sites (Levine et al., 2018), Hannum's clock based on 71 CpG
241 sites (Hannum et al., 2013), the Lu telomere length predictor, and DNA methylation based mortality
242 risk assessment (GrimAge (Lu et al., 2019)) using the Horvath online calculator. However, we found
243 large bidirectional fluctuations in epigenetic age up to 8.99 years for DNAmAge, 4.49 years for
244 Horvath skin-and-blood, 7.94 years for DNAmPheno Age, 6.25 years for Hannum's clock, and 4.03
245 years for GrimAge that did not seem to be related to COVID-19 infection **Supplementary Figure S4**.
246 Instead, this appeared to be attributable to widespread technical noise in DNAm measurement (Bose
247 et al., 2014; Logue et al., 2017; Sugden et al., 2020), as previous studies have found that repeated

248 measurements of the same sample to deviate up to 9 years (Higgins-Chen et al., 2021b). To mitigate
249 the impacts of these unreliable epigenetic clock estimates, we applied a novel principal-component
250 version of epigenetic clocks that permits a more reliable estimate for longitudinal studies (Higgins-
251 Chen et al., 2021b). Next, we applied the principal-component epigenetic clocks algorithm based on
252 78,464 CpGs to the dataset to obtain PC-based epigenetic clock estimates and PC-based residuals after
253 regressing PC-age predicted by the algorithm over chronological age for participants prior to and
254 following COVID-19. Since age is a well-known risk factor for COVID-19 severity and our sample
255 set contained participants that ranged in chronological age from 18 to 73 years, we stratified our
256 longitudinal analysis of epigenetic clocks into two groups: people under 50 and people over 50 years
257 of age. Application of our novel principal component-based computational solution to optimize the
258 aging signal from epigenetic clocks and minimize noise revealed no significant differences in
259 epigenetic age based on the PCHorvath1, PCHorvath 2, and PCHannum epigenetic clocks for both
260 groups following COVID-19 (**Fig.4a-c**). Additionally, PCDNAMTL was not significantly altered
261 following COVID-19 (**Fig.4d**). We observed that the PCPhenoAge clock was significantly increased
262 in those over 50 years of age following COVID-19 by an average of 2.1 years (**Fig.4e,h**). In contrast
263 to the observations for those over 50 years of age, PCPhenoAge was significantly decreased in those
264 under 50 years of age following COVID-19 by an average of 2.06 years (**Fig.4g**). Chronological age
265 significantly related to the extent of pre- vs post-COVID-19 epigenetic age increase in PCPhenoAge
266 (**Fig.4i**). Moreover, we observed that PCGrimAge, a predictor of lifespan in unit of years was
267 significantly increased in people over 50 years of age following COVID-19 by an average of 0.84 years
268 (**Fig.4f,k**). Chronological age significantly related to the extent of pre- vs post-COVID-19 epigenetic
269 age increase in PCGrimAge (**Fig.4l**). PCGrimAge was not significantly impacted in those under 50
270 years of age (**Fig.4j**).

271 We hypothesized that the COVID-19 associated change in PCPhenoAge and PCGrimAge was
272 related to immune cell type compositional changes. Indeed, we observed that the increase in the
273 PCPhenoAge clock estimate for participants following COVID-19 was significantly related to the
274 magnitude of changes in the percent of CD4 T cells, B cells, Granulocytes, plasmablasts, exhausted T
275 cells, CD8 naïve T cells, and CD4 naïve T cells (**Fig.5**). We did not observe significant relationships
276 between the increase in PCPhenoAge and CD8T cells, NK cells, and monocytes (**Fig.5**). Moreover,
277 we identified that the extent of increase in PCGrimAge estimates for participants following COVID-
278 19 was significantly related to blood immune cell compositional changes in CD4 T cells, NK cells, B
279 cells, granulocytes, and plasmablasts (**Fig.5**). The loss in percent CD4+ T cells following COVID-19
280 for all participants significantly related to older chronological age and increasing epigenetic age
281 inferred from all epigenetic clocks (PCHorvath1, PCHorvath2, PCHannum, PCPhenoAge, and
282 PCGrimAge) (**Fig.5**), supporting observations of lymphopenia related to COVID-19. Together, these
283 findings suggest that the epigenetic aging signal related to COVID-19 exposure is driven by changes
284 in blood immune cell type composition. We also examined whether COVID-19 impacted measures
285 from a DNA methylation-based mitotic clock (“epiTOC” (Yang et al., 2016)) and quantification of
286 the pace of biological aging (“DunedinPoAm” (Belsky et al., 2015, 2020)) and observed no significant
287 differences pre vs post-COVID-19 in these measures (**Supplementary Figure S5**).

288

289 **2.6 mRNA COVID-19 vaccination in older individuals decreases epigenetic age and may** 290 **reflect age-related B- cell and plasmablasts induction and expansion**

291 To complement our pre- and post-COVID-19 exposure dataset, we sought to examine the
292 impact of mRNA COVID-19 vaccination upon epigenetic clocks by obtaining DNA methylation
293 profiles from blood of participants prior to and following mRNA COVID-19 vaccination. We
294 examined 36 individuals (n=21 Females; n=15 Males) ranging in age from 22 to 69 years old that

295 received either the Moderna (n=13) or Pfizer (n=23) mRNA vaccine. The median time since the
296 second mRNA vaccine dose received by participants and DNA methylation data obtained for the
297 post-vaccination timepoint was 57.9 days. We calculated principal-component epigenetic clock
298 estimates and observed that PCHorvath1 and PCHorvath2 epigenetic age estimates were significantly
299 decreased following complete mRNA vaccination comparing pre- and post-vaccination timepoints
300 for all 36 participants by an average of 1.03 years and 1.58 years (**Fig.6a,b**). Exploratory analyses
301 stratified by vaccine brand suggested that those over 50 years of age that received Moderna mRNA
302 vaccination significantly reduced epigenetic age estimates based on PCHorvath1 by an average 2.75
303 years and PCHorvath2 by an average 3.91 years following complete vaccination (**Fig.7a,b**). In
304 contrast, we observed no significant differences in epigenetic age estimates for people under 50 that
305 received Moderna and for both those under and over 50 years of age that received Pfizer
306 (**Fig.7a,b,g,h**). Whether these stratified results relate to Moderna vaccine containing a higher dose
307 (100 micrograms) compared to Pfizer (30 micrograms) will need further examination. There was no
308 significant difference in time from last dose and when DNA methylation data was obtained post-
309 vaccination between vaccine brands (**Supplementary Figure S6**), suggesting time was not a
310 confounding factor for vaccine differences in epigenetic age reduction in those over 50 years of age.
311 In correlative analyses for all participants receiving an mRNA vaccine, we observed the extent of
312 decreasing epigenetic age based on the PCHorvath1 and PCHorvath2 clocks and increasing
313 PCDNA_mTL significantly related to increasing chronological age (**Fig.7m,n,q**). We did not observe
314 any significant differences from mRNA vaccination upon the PCHannum, PCPhenoAge, and PC
315 DNA_mTL(**Fig.7c,d,e,i,j,k**) and delta epigenetic age changes for PCHannum, PCPhenoAge, and PC
316 GrimAge were not significantly related to chronological age (**Fig.7o,p,r**).

317 Next, we examined whether the decrease in PCHorvath1 and PCHorvath2 following mRNA
318 vaccination related to immune cell type compositional changes and/or DNA methylation inferred

319 telomere length since previous data suggested telomere length related to influenza vaccine responses
320 (Najarro et al., 2015). The delta change in PCHorvath1 following mRNA vaccination significantly
321 associated with delta change in PCDNA_mTL and plasmablasts cell type percentage following
322 complete two dose mRNA vaccination (**Fig.8**). The delta change in PCHorvath2 following mRNA
323 vaccination significantly associated with delta change in PCDNA_mTL, B cell, granulocytes, and
324 plasmablasts following complete two dose mRNA vaccination (**Fig.8**). Notably, we did not observe
325 any significant relationships between the time elapsed from when participants received their second
326 mRNA dose and post mRNA vaccine DNA methylation data was obtained and delta changes in all
327 epigenetic clock estimates and cell type compositional changes following mRNA vaccination (**Fig.8**).

328 **2.7 Short-term SARS-CoV-2 infection and exposure *in vitro* does not substantially impact** 329 **epigenetic clocks.**

330 We tested whether artificial short-term *in vitro* exposure to SARS-CoV-2 virus (0.1 MOI)
331 impacted PC-based epigenetic clocks in human peripheral mononuclear cells. We exposed viable
332 PBMC's from two uninfected donors (Donor 1, under 50 years of age; Donor 2: over 50 years of age)
333 to a passage 4 stock of SARS-CoV-2 (0.1 MOI) *in vitro* for 60 hrs and compared DNA methylation
334 levels to mock uninfected. We did not observe evidence of SARS-CoV-2 replication in PBMCs after
335 60 hrs as assessed by nucleocapsid flow cytometry assessments. PC-based epigenetic estimates of
336 difference in epigenetic age comparing mock and SARS-CoV-2 exposed PBMC revealed changes
337 less than 1 year for PCHorvath1, PCHorvath2, and PCHannum clocks (**Supplementary Figure S7**).
338 Notably, we observed divergent donor-dependent impacts from addition of monophosphoryl lipid A
339 (MPLA) stimulation, a TLR4 agonist, for 1 hr to 60hr SARS-CoV-2 exposed PBMC's for all PC-
340 based clocks (**Supplementary Figure S7**). As a comparator dataset, we generated DNA methylation
341 data from mock and SARS-CoV-2 infected Calu-3 cells for 96 hours and observed epigenetic age did
342 not increase for PC-based epigenetic clock comparing mock and infected cells.

343 **Discussion**

344 In this pilot study, we examined whether SARS-CoV-2 infection and mRNA COVID-19
345 vaccination impacted DNA methylation states and epigenetic clocks in healthy individuals in the
346 short term. Our findings revealed that significant differences in DNA methylation in blood associate
347 with SARS-CoV-2 infection at 756 CpG sites, suggesting an immune cell-based epigenetic signature
348 of COVID-19 may derive from aberrant DNA methylation states related to immune dysfunction
349 induced by COVID-19. These findings support epigenetic findings from other groups that have
350 reported distinct DNA methylation states in blood as a potential biomarker of COVID-19 (Balnis et
351 al., 2021; Castro de Moura et al., 2021; Zhou et al., 2021). Moreover, our epigenetic clock findings
352 reveal an age-related impact of epigenetic age increase associated with natural SARS-CoV-2
353 infection on the PCPhenoAge epigenetic clock and mortality risk estimate PCGrimAge in
354 mild/moderate cases. Whether the extent and durability of this perturbation to these two epigenetic
355 clock estimates is related to long COVID-19 or long-term aging outcomes remains an intriguing area
356 for further investigation.

357 In contrast to natural SARS-CoV-2 infection, we observed that two epigenetic clocks
358 (DNAmAge/PCHorvath1 and DNAmAgeSkinBlood/PCHorvath2) were decreased following mRNA
359 COVID-19 vaccination in individuals over 50. The extent of decreased epigenetic age following
360 mRNA-COVID-19 vaccination significantly related to changes in B cells and plasmablasts,
361 highlighting the potential utility of epigenetic clocks in capturing vaccine responses and tracking the
362 need for booster shots due to waning COVID-19 immunity in older individuals. These results are
363 more robust because multiple clocks that putatively measure the same aging phenotype (i.e.
364 PCGrimAge and PCPhenoAge predict mortality risk, while PCHorvath1 and PCHorvath2 track with
365 chronological age) show similar relationships to COVID-19. Together, this pilot longitudinal
366 epigenetic dataset of natural COVID-19 exposure and mRNA COVID-19 vaccination has important
367 implications for research into the impact of COVID-19 on aging and the potential for mRNA

368 vaccination to impact epigenetic aging in the immune system. Future research will need to examine
369 whether COVID-19 and mRNA vaccine-related changes to epigenetic age are biologically
370 meaningful. It is important to note that although epigenetic age robustly predicts age-related
371 morbidity and mortality in cross-sectional studies (Horvath and Raj, 2018; Oblak et al., 2021), it is
372 unknown if modifying epigenetic age in the short term leads to changes in long-term outcomes.

373 Prior research has shown that the host epigenetic landscape is altered during coronavirus
374 infection (Schäfer and Baric, 2017). Evidence indicates that SARS-CoV-2 infection has a substantial
375 impact upon the host immune cell epigenetic and transcriptional landscape in severe COVID-19
376 (Corley et al., 2021; Rendeiro et al., 2021). Our findings support a recent cross-sectional human
377 DNA methylation study of COVID-19 that reported DNA methylation patterns of COVID-19
378 convalescents compared to uninfected controls (Huoman et al., 2021). In addition, our study provides
379 the first examination of longitudinal DNA methylation changes in blood of healthy participants prior
380 to and following test-confirmed mild/moderate COVID-19. We observed blood-based DNA
381 methylation changes associated with COVID-19 exposure in healthy participants ranging in age with
382 261 differentially methylated CpGs identified. Among the COVID-19 differentially methylated loci
383 we detected in blood, we observed hypermethylation related to the caspase recruitment domain
384 family member 14 (*CARD14*) gene. This gene encodes a protein that has been shown to interact with
385 BCL10 that functions as a positive regulator of cell apoptosis and NF-kappaB activation (Bertin et
386 al., 2001). Moreover, *CARD14* may play a role in protecting cells against apoptosis. We observed
387 that the percent change in DNA methylation inferred immune cell type proportion for CD8 T cells for
388 participants following COVID-19 exposure significantly associated with the DNA methylation
389 percent change related to *CARD14*. This suggest that a subset of DNA methylation changes related to
390 COVID-19 exposure were due to cell type compositional changes. Notably, we also observed the
391 differentially methylated CpGs associated with COVID-19 were enriched in transcriptional gene sets

392 identified from published SARS-CoV-2 human, animal model, and *in vitro* infection studies
393 (Kuleshov et al., 2016, 2020). These findings suggest that DNA methylation changes associated with
394 COVID-19 likely participate in the regulation and modulation of host gene expression from infection.
395 Together, this first set of findings support the notion that distinct host DNA methylation states in
396 circulating immune cells serves as a COVID-19 specific epigenetic signature. The durability of this
397 COVID-19 epigenetic signature remains a key question for future study.

398 Recent work utilizing a cross sectional study design reported that epigenetic clocks are not
399 altered in COVID-19 (Franzen et al., 2021). Our work contrasts with this report and suggests that
400 specific epigenetic clocks may be altered by COVID-19 based on age. We utilized a more powerful
401 longitudinal study design of individuals prior to and following test-confirmed COVID-19 and applied
402 a novel principal component-based assessment of epigenetic clocks that mitigates issues with
403 reliability in standard epigenetic clock algorithms. We observed a divergence in the epigenetic clock
404 estimate PCPhenoAge and epigenetic clock mortality algorithm PCGrimAge based on age in
405 individuals following COVID-19. Slight epigenetic age acceleration in the short term appeared in
406 those individuals over 50 years of age that were infected with SARS-CoV-2. In contrast, epigenetic
407 age appeared to reduce in those individuals under 50 years of age following COVID-19.

408 PCPhenoAge and PCGrimAge are among the strongest epigenetic predictors of mortality risk
409 (Levine et al., 2018; Lu et al., 2019; Higgins-Chen et al., 2021a). These findings support the critical
410 role of age as a COVID-19 risk factor and suggest that specific epigenetic clocks can capture an age-
411 dependent perturbation to epigenetic clocks following COVID-19. Moreover, prior multi-omic
412 analysis has shown that the Levine clock accelerates with cellular senescence and mitochondrial
413 dysfunction (Liu et al., 2020). Prior studies of epigenetic clocks in COVID-19 utilized different sets
414 of clocks which may explain their conflicting results (Corley et al., 2021; Franzen et al., 2021;
415 Mongelli et al., 2021a). Interrogating a wide array of clocks simultaneously is essential for
416 determining which clocks are most related to COVID-19 or vaccination. Furthermore, findings are

417 more robust if multiple clocks predicting the same phenotype show the same relationship to COVID-
418 19.

419 A plausible interpretation of the PCPhenoAge/PCGrimAge results after infection is an age-
420 related signal of both immunosenescence and inflammaging. Once the immune system is activated
421 in younger individuals by SARS-CoV-2 infection, they look younger by the epigenetic clock due to a
422 robust activation of the immune response that reflects younger individuals (not that they are actually
423 becoming younger). In older individuals, activation of non-specific inflammatory pathways after
424 SARS-CoV-2 infection appears to increase epigenetic age because of the activation of pathways that
425 overlap/are similar to inflammaging. An alternative interpretation for divergence in epigenetic age
426 based on age during SARS-CoV-2 infection might involve the biological process of hormesis:
427 moderate stressors can improve health by causing a compensatory response (Epel, 2020). COVID-19
428 might serve as a hormetic stress in non-hospitalized younger individuals, while it serves as a toxic
429 stressor in older adults or any severe case.

430 Aging drives immunosenescence with implications for a decline in adaptive immunity
431 resulting in reduced vaccine responses and vaccine durability in older adults. The age-related decline
432 in immune function including reduced thymic output of naïve T cells and dampened B cell
433 generation has notably led to decreased vaccine efficacy in older individuals (Soiza et al., 2021).
434 Indeed, building evidence for COVID-19 indicates a declined humoral and cellular immune response
435 in older individuals (Collier et al., 2021; Levin et al., 2021). Yet, failure to achieve a protected or
436 durable response after vaccination is poorly understood despite occurring commonly among many
437 elderly individuals. Our epigenetic clock data following mRNA COVID-19 vaccination revealed an
438 age-related decrease in epigenetic age following vaccination. Our findings also revealed that the
439 change in epigenetic age following vaccination was specifically related to immune-cell type
440 compositional changes in the percentage of B cells, plasmablasts, and granulocytes. These findings

441 support work showing that SARS-CoV-2 mRNA vaccines induce persistent germinal center B cell
442 response that enables robust humoral immunity (Turner et al., 2021). Our findings do not provide any
443 insights into the particular impact of the mRNA lipid nanoparticle compared to the expressed spike
444 protein upon different epigenetic clocks. These compelling findings suggest that epigenetic profiles
445 and specifically epigenetic clock estimates may provide insights into individual and age-related
446 humoral immune responses to COVID-19 vaccination. Previous work has shown the impact of
447 influenza vaccination on persistent epigenomic remodeling of immune cells (Wimmers et al., 2021)
448 and explored the idea of whether epigenetic age could relate to vaccine responses in the context of
449 influenza (Gensous et al., 2018).

450 Recent work examining T cell exhaustion after recovery from chronic infection in humans has
451 found that epigenetic scars of CD8+ T cell exhaustion persists in humans (Yates et al., 2021),
452 suggesting indelible imprints on the host immune cell epigenome from viral infection. The
453 hypothesis of a persistent epigenetic dysregulation of host immune cells contributing to long-
454 COVID-19 remains unclear. Whether durable changes to epigenetic clocks are reflected by
455 epigenetic scars of particular immune cell types and relate to long-COVID-19 is a compelling
456 hypothesis to pursue.

457 Our findings highlight the benefits of our computational solution using principal components
458 for calculating PC-based epigenetic clocks for longitudinal studies (Higgins-Chen et al., 2021b).
459 Using standard epigenetic clock estimates, we observed variation up to 9 years in participants pre-
460 and post-timepoint samples epigenetic age estimates for all clocks that lead to non-significant results.
461 While the application of PC-based epigenetic clocks pulled out a biological signal suggesting that
462 mild/moderate COVID-19 from SARS-CoV-2 infection and mRNA vaccination impacted epigenetic
463 clocks, the biological mechanisms that influence detrimental or beneficial changes in epigenetic
464 clocks remains unclear. Ongoing research is deconstructing dissimilar epigenetic clocks and may

465 provide further insights into the precise biological mechanisms captured from age-related alterations
466 in the methylation landscape during infection and mRNA vaccination.

467 The developed mRNA vaccines for COVID-19 have been shown to elicit a potent humoral
468 immune response and be highly efficacious at preventing COVID-19 and severe disease outcomes
469 (Polack et al., 2020; Baden et al., 2021; Tartof et al., 2021). Our DNA methylation dataset was
470 obtained at a median post second dose of around 2 months. Based on data showing durability of
471 vaccine responses out to 6 months post-vaccination (Doria-Rose et al., 2021), our DNA methylation
472 data was captured during an effective post-vaccine time frame window. Future studies will need to
473 harness serial sample collection of participants during the course of mRNA vaccination and assess
474 critical time points for impacts of mRNA vaccination upon epigenetic clocks. Moreover, our
475 observations of age-related impacts from mRNA vaccination upon epigenetic age warrants further
476 investigation to determine whether this measure may be relevant to age-related waning vaccine
477 effectiveness. Lastly, epigenetic age assessments of participants that received heterologous prime-
478 boost vaccination against COVID-19 (Borobia et al., 2021; Nordström et al., 2021; Pozzetto et al.,
479 2021; Schmidt et al., 2021; Shaw et al., 2021) and heterologous booster vaccinations (Atmar et al.,
480 2021) should be studied.

481 Considering the challenges with longitudinal blood collection and acquisition of epigenetic DNA
482 methylation data from participants at timepoints prior to and following test-confirmed COVID-19, all
483 of the published COVID-19 DNA methylation studies have been cross-sectional study designs
484 (Bernardes et al., 2020; Balnis et al., 2021; Castro de Moura et al., 2021; Corley et al., 2021).
485 Longitudinal epigenetic studies are considered the gold standard study design to mitigate
486 interindividual variation in DNA methylation patterns and track environmental and pathogen-induced
487 changes to the epigenome (Chen et al., 2018). Hence, our assessment of longitudinal DNA methylation
488 of 21 participants provides a discovery dataset for examining the short-term impacts of COVID-19

489 upon the host immune cell epigenome and impact on epigenetic clock estimates. Our longitudinal
490 COVID-19 DNA methylation dataset consisted of healthy participants that ranged across the lifespan
491 from 18 to 73 years of age. Moreover, the collection of DNA methylation data following test-confirmed
492 COVID-19 exposure occurred within a short-term time frame of a 6-month window and occurred early
493 during the COVID-19 pandemic reflecting infection with a less evolved, less contagious, and
494 potentially less severe SARS-CoV-2 virus than recent variants such as the Delta variant. Hence, our
495 findings are limited by these potential factors. These longitudinal findings need to be confirmed in a
496 larger sample size, across diverse regions and genotypes, among individuals across the lifespan, in
497 people infected with emerging SARS-CoV-2 variants, and across COVID-19 severities including those
498 individuals that recover and suffer from long-lasting symptoms termed post-COVID.

499 Despite the strengths of this longitudinal epigenetic study, there are several limitations. First,
500 our longitudinal study design only included two time points to examine changes related to COVID-
501 19 and mRNA vaccination comparing baseline and a short-term follow-up assessment of DNA
502 methylation. future studies will need to study a larger sample size and determine whether these age-
503 related divergent changes to epigenetic clocks are durable following COVID-19 and potentially relate
504 to those with long-COVID-19 syndrome. Additionally, there was variation in the time following
505 confirmed COVID-19 or mRNA COVID-19 vaccination for when the post sample assay for DNA
506 methylation was completed. Yet, given the complete lack of longitudinal DNA methylation studies of
507 COVID-19 and mRNA COVID-19 vaccination we provide discovery findings that are compelling
508 regarding specific DNA methylation changes and epigenetic clocks that warrant further investigation.
509 Future studies that have serial blood collection of participants throughout the course of mRNA-
510 vaccination and even following booster shots will be extremely valuable for epigenetic clock
511 investigations. Recent technological advancements based on Tagmentation-based Indexing of
512 Methylation Sequencing (TIME-Seq) have scaled and reduced the cost of epigenetic age predictions

513 permitting methodology for a more comprehensive study follow-up to our findings (Griffin et al.,
514 2021). We also acknowledge the limited clinical data for participants and that the SARS-CoV-2
515 infection DNA methylation dataset may be relevant to a early genetic lineage not reflecting emerging
516 variants being monitored nor variants of concern such as Delta (B.1.617.2) .

517

518 **3 Methods**

519 **3.1 Study Cohort**

520 Deidentified DNA methylation data was generated by TruDiagnostic as part of a retrospective non-
521 randomized study to assess the effects of SARS-CoV-2 infection and mRNA vaccination upon DNA
522 methylation patterns. Participants post-COVID-19 sample DNA methylation was test confirmed PCR
523 testing or serology testing and occurred between August 2020 and March 2021. This study was
524 approved by the Institute of Regenerative and Cellular Medicine IRB and Weill Cornell Medicine
525 IRB.

526 **3.2 DNA methylation Assessment**

527 Peripheral whole blood was collected by lancet and capillary method into lysis buffer and DNA
528 extracted. 500 ng of DNA were bisulfite converted using the EZ DNA Methylation kit (Zymo
529 Research) according to the manufacturer's instructions. Bisulfite-converted DNA samples were
530 randomly assigned to a chip well on the Infinium HumanMethylationEPIC BeadChip, amplified,
531 hybridized onto the array, stained, washed, and imaged with the Illumina iScan SQ instrument to
532 obtain raw image intensities. DNA methylation data for longitudinal sampling of participant's pre-
533 and post-COVID-19 and pre- and post-vaccination time points was assayed for each participant at
534 separate times.

535 **3.3 DNA methylation analyses**

536 Raw Methylation EPIC array IDAT intensity data was loaded and preprocessed in the R statistical
537 programming language (<http://www.r-project.org>) using The Chip Analysis Methylation Pipeline
538 (ChAMP, version 2.8.3)(Tian et al., 2017). IDAT files were loaded using the champ.load function.
539 All samples passed quality control metrics. Comprehensive filtering was applied to the dataset for
540 probes with detection P-values <0.01, all non-CpG probes, previously published SNP-related probes,
541 multi-hit probes, and probes on sex chromosomes. Methylation beta-values ranging from 0 -1
542 (corresponding to unmethylated to methylated signal intensity) for each sample were normalized
543 using the BMIQ function implemented in the ChAMP pipeline. DNA methylation epigenetic age
544 parameters were calculated using Horvath's web-based DNAm age calculator tool(Horvath, 2013; Lu
545 et al., 2019). Cell type deconvolution estimates for blood were calculated using the EpiDISH
546 package(Zheng et al., 2019). To identify differentially methylated loci, we utilized an FDR
547 adjustment (Benjamini-Hochberg) and adjusted P value cutoff at 0.05 to compare participants pre-
548 COVID-19 methylation data to post-COVID-19 methylation data. Genes related to differentially
549 methylated loci were utilized for a COVID-19 gene set analyses from the Enrichr web tool(Kuleshov
550 et al., 2016).

551 **Epigenetic Clock Analysis and Estimating blood immune cell type composition.**

552 Epigenetic clock estimates, DNA methylation-based cell type deconvolution proportions, and
553 epigenetic biomarkers were calculated using the online calculator (<https://dnamage.genetics.ucla.new>).
554 Principal component-based epigenetic clock estimates were calculated utilizing an R script and 78,464
555 CpGs for each sample in a beta matrix. Mean imputation was utilized for missing values. Pace of aging
556 was calculated utilizing the DunedinPACE algorithm (DunedinPoAm_45). To calculate pace of aging,
557 noob-normalized and masked beta values were first processed from raw IDAT files using the Sesame
558 R package(Zhou et al., 2018). To limit the number of batch effects caused by processing multiple bead
559 chips, individual bead chips were processed at a time to generate the normalized beta values and then
560 used to quantify pace of aging. The pace of aging metric was then calculated using the DunedinPACE
561 algorithm described in Belsky et al. 2021(Belsky et al., 2021). Briefly, the algorithm uses 19 different
562 physiological biomarkers to generate overall pace of aging from the Dunedin Study cohort (N = 1037).
563 A standardized average rate of aging is then regressed using an elastic net regression model against
564 methylation values generated from blood collected from the cohort at the age of 45, which identified
565 173 CpG sites that are associated with the pace of aging metric. The DunedinPACE algorithm was
566 used to calculate the pace of aging measure obtained from authors. Analyses were performed in R 4.1.1
567 and RStudio Version 1.4.1717. Figures were made using GraphPad and corrplot R package.

568 ***In vitro* SARS-CoV-2 infection and exposure:** SARS-CoV-2 virus (isolate USA-WA1/2020 (BEI
569 resources; NR-52281) was propagated and titrated in Vero E6 cell lines. De-identified donor PBMC
570 specimens were obtained from Astarte Biological for *in vitro* exposure to 0.1 MOI SARS-CoV-2 for
571 60 hrs. Calu-3 cells were infected for 96 hrs.

572

573

574

575

576

577

578

579

580

581

582

583

584

585

586 4 Figure Legends

587 **Figure 1. DNA methylation changes in blood associated with mild/moderate COVID-19.**

588 **a.** Study design of longitudinal assessment of DNA methylation profiles in 21 participants pre- and
589 post-SARS-CoV-2 infection. **b.** Manhattan plot of differentially methylated loci (DML) associated
590 with mild/moderate COVID-19. **c.** Bar graph of genomic enrichment of COVID-19 DML in 13
591 different categorized regions of the genome relative to gene and CpG island. Hypergeometric test
592 utilized to calculate P value and odd ratio. **d-m.** Plots of COVID-19 DML displaying mean DNA
593 methylation levels +/- SEM for CpGs associated with a gene ID. Adjusted P value calculated
594 utilizing Benjamini-Hochberg correction.

595 **Figure 2. DNA methylation inferred blood immune cell type composition following**

596 **mild/moderate COVID-19. a-j.** Plots displaying the change in specific immune cell type
597 populations inferred from DNA methylation in individuals pre- vs post-COVID-19 stratified by age.
598 Triangles display participants under 50 years of age and circles display participants over 50 years of
599 age.

600 **Figure 3. DML associated with COVID-19 relate to immune cell type composition.** Correlogram
601 plot of biological age, the change in DNA methylation levels for COVID-19 related DML, and the
602 change in inferred immune cell type following COVID-19. Significant correlations displayed as solid
603 box and Spearman's rank correlation coefficient displayed.

604 **Figure 4. Divergence in principal component-based DNAmPhenoAge and GrimAge mortality**
605 **risk increased based on age related to COVID-19. a-f.** Plots displaying the change in principal
606 component-based epigenetic clock age estimates in individuals pre- vs post-COVID-19 stratified by
607 age. Triangles display participants under 50 years of age and circles display participants over 50
608 years of age. **g-h.** Plots displaying the change in principal component-based PhenoAge in individuals
609 under and over 50 years of age pre- vs post-COVID-19. **i.** Correlation plot of chronological age and
610 the change in PCPhenoAge pre- vs post-COVID-19. **j-k.** Plots displaying the change in principal
611 component-based GrimAge in individuals under and over 50 years of age pre- vs post-COVID-19. **l.**
612 Correlation plot of chronological age and the change in PCGrimAge pre- vs post-COVID-19.

613 **Figure 5. COVID-19 related epigenetic clock changes associate with immune cell type changes.**
614 Correlogram plot of biological age, the change in PC-based epigenetic clocks pre- vs. post-COVID-
615 19, and the change in inferred immune cell type following COVID-19. Significant correlations
616 displayed as solid box and Spearman's rank correlation coefficient displayed.

617 **Figure 6. mRNA COVID-19 vaccination decreases PCHorvath1 and PCHorvath2 epigenetic**
618 **age. a.** Longitudinal plot of individuals PCHorvath1 and **b.** PCHorvath2 epigenetic age at pre-
619 vaccine and post-mRNA vaccination time points. Paired t-test P value displayed.

620 **Figure 7. Moderna mRNA COVID-19 vaccination decreases principal component-based**
621 **epigenetic age in individuals over 50. a-f.** Plots displaying the change in principal component-based
622 epigenetic clock age estimates in individuals pre- vs post-mRNA Moderna vaccination stratified by
623 age. Triangles display participants under 50 years of age and circles display participants over 50
624 years of age. **g-i.** Plots displaying the change in principal component-based epigenetic clock age
625 estimates in individuals pre- vs post-mRNA Pfizer vaccination stratified by age. **m-r.** Correlations
626 between chronological age and pre- vs. post- mRNA vaccination change in PC-based epigenetic
627 clock estimates.

628

629 **Figure 8. mRNA vaccine-related epigenetic clock changes associate with immune cell type**
630 **changes.** Correlogram plot of time since 2nd dose, the change in PC-based epigenetic clocks pre- vs.
631 post-COVID-19, and the change in inferred immune cell type following COVID-19. Significant
632 correlations displayed as solid box and Spearman's rank correlation coefficient displayed.

633

634 **5 Conflict of Interest**

635 *The authors declare that the research was conducted in the absence of any commercial or financial*
636 *relationships that could be construed as a potential conflict of interest.*

637

638

639 **6 Tables**

640 **Table 1**

	Pre-COVID-19	Post-COVID-19
Age (year) ^a	46.07 (18.53, 73.03)	46.54 (19.41, 73.66)
Sex (male, %)	14 (66.67%)	-
Time before COVID-19 Diagnosis DNAm assayed (Weeks)	19.39 (4.35, 49.83)	-
Time after COVID-19 Diagnosis DNAm assayed (Weeks)	-	8.35 (1.00, 27.10)
PCR Test Confirmed (%)	-	85.71%
Antibody Test Confirmed (%)	-	14.29%

641 ^aData are median (Minimum, Maximum)

642

Table 2: Differentially Methylated Loci Overlapping with Enrichr COVID-19 Related Gene Sets 2021

Term	Overlap	Adjusted P-Value	Combined Score	Genes
Top 500 down genes for SARS-CoV-2 infection in Rhesus macaques at Group 2 dose in PBMCs at 10 DPI from GSE156701	28/470	0.017	25.08	<i>DGKG; MAST4; TRRAP; EHMT2; MAST2; PRR3; ATP2A3; ZBTB20; DTX1; TRAK1; SIPA1L3; SYNE2; LOXHD1; UNK; NACC1; ZNF764; DST; USP42; ATP8B1; IQSECI; AIG1; KLF16; SLC5A6; NCOR2; HIC2; RAPGEF1; RIN3; PPARA</i>
Top 500 upregulated genes in mouse heart with SARS-CoV-2 infection (Day 7) from GEO GSE162113	26/439	0.018	23.08	<i>TRRAP; EHMT2; ANKRD11; AP2A1; CHD4; MLLT6; SLC2A8; AKAP13; NCLN; MYO18A; FBRSL1; HMGXB3; PCNT; FNBP4; PDCD6IP; SEC16A; INSR; NBEAL2; TADA2B; NCOR2; HIC2; MLXIPL; UBE2O; ACIN1; FAM193B; ALDH9A1</i>
Top 500 down genes for SARS-CoV-2 infection in Mesocricetus auratus hamster blood Day 14 from GSE162208	24/404	0.021	21.68	<i>GGT5; ABCC1; COL27A1; PDCD6IP; TRRAP; IQSECI; SEC16A; AP3D1; NBEAL2; ATP11A; GMIP; HIPK1; TRAK1; SSH2; SLC2A6; NCSTN; NOL4L; MAPK7; NFKBIZ; HIVEP3; TNRC18; CDK12; ASCC3; UGGT1</i>
Top 500 up genes for SARS-CoV-2 late-stage infection in human female blood from GSE161731	27/497	0.027	18.57	<i>TTC22; ATP2A3; SLC2A1; MLLT6; ADAMTS14; RXRA; MAPK7; MYO18A; FBRSL1; TNRC18; INTS1; IQSECI; AP3D1; TBCD; WWP2; EPS15L1; LSS; NCOR2; SLC7A5; SP2; RAPGEF1; TUBGCP6; UBE2O; CDK12; LZTR1; PLCD1; PFKP</i>
Top 500 upregulated genes in mouse spleen with SARS-CoV-2 infection (Day 7) from GEO GSE162113	24/425	0.027	18.78	<i>SCARB1; INTS1; MAST4; EHMT2; IGHMBP2; IQCE; NBEAL2; AP2A1; GMIP; TRAK1; MEIS3; SIPA1L3; MLLT6; NCOR2; ADAMTS14; UNK; NCLN; MAPK7; SLIT1; FBRSL1; ACIN1; TNRC18; FAM193B; SASH1</i>
500 genes up-regulated by SARS-CoV-2 in human Calu3 cells at 4h from GSE148729 mock totalRNA	26/487	0.030	17.06	<i>ROCK1; TRRAP; SPG7; FOXO1; MED12L; GOLGA3; AKAP13; PCLO; NFKBIZ; MYO18A; HMGXB3; ZNF764; KCTD19; JAG1; INTS1; SEC16A; INSR; NBEAL2; PILRB; ASH1L; ATP11A; SSH2; TIAM2; SLC7A5; UBE2O; FGFR1</i>
Top 500 upregulated genes for SARS-CoV-2 infection in human cornea from GSE164073	25/470	0.032	16.31	<i>NUMBL; ZBTB47; ITGB3; NPAS2; SNX29; RASSF4; FAM110B; KIAA1522; PDPN; NFKBIZ; ZNF423; SYBU; PLXNA4; ABCC1; JAG1; RBPMS; ACSL1; IQSECI; FOXN3; LSS; TIAM2; ARHGAP32; SDK1; NEK10; GAS7</i>

500 genes up-regulated by SARS-CoV-2 in A549-ACE2 cells from GSE154613 trifluoperazine	25/471	0.032	16.21	<i>NUMBL; TCF25; EHMT2; ANKRD11; AP2A1; SIPA1L3; ERICH1; FASTK; NACCI; TNRC18; COL27A1; INTS1; TPM2; TALDO1; TBCA; MEIS3; KLF16; NCOR2; COL5A1; MMP17; TRIP10; ACIN1; BCAR1; PFKP; EIF4G1</i>
--	--------	-------	-------	---

644

645

646

647

648

649

650

651

652

653

654

655

656

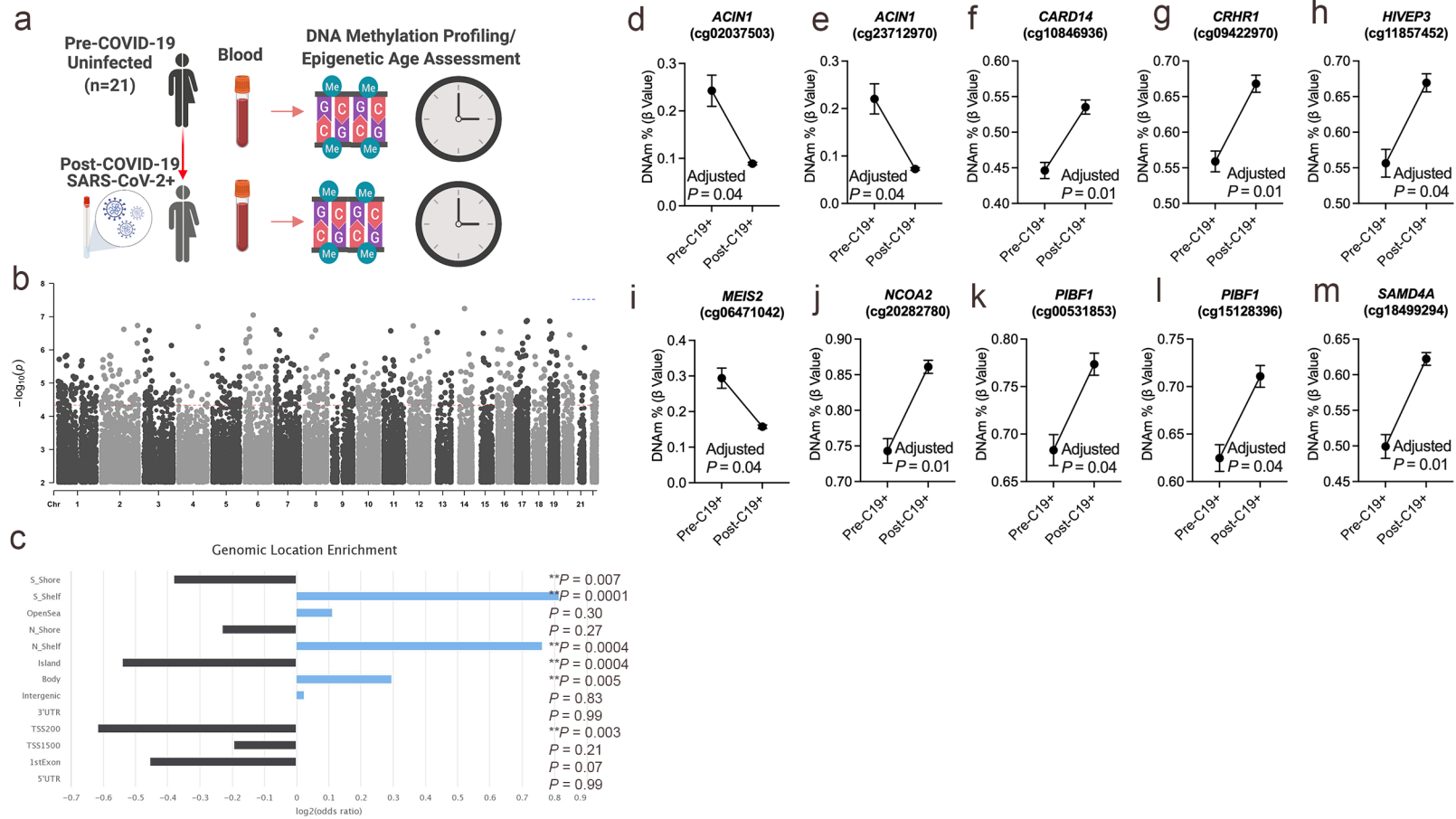
657

658

659

660

661 **Figure 1. DNA methylation changes in blood associated with mild/moderate COVID-19.**



662

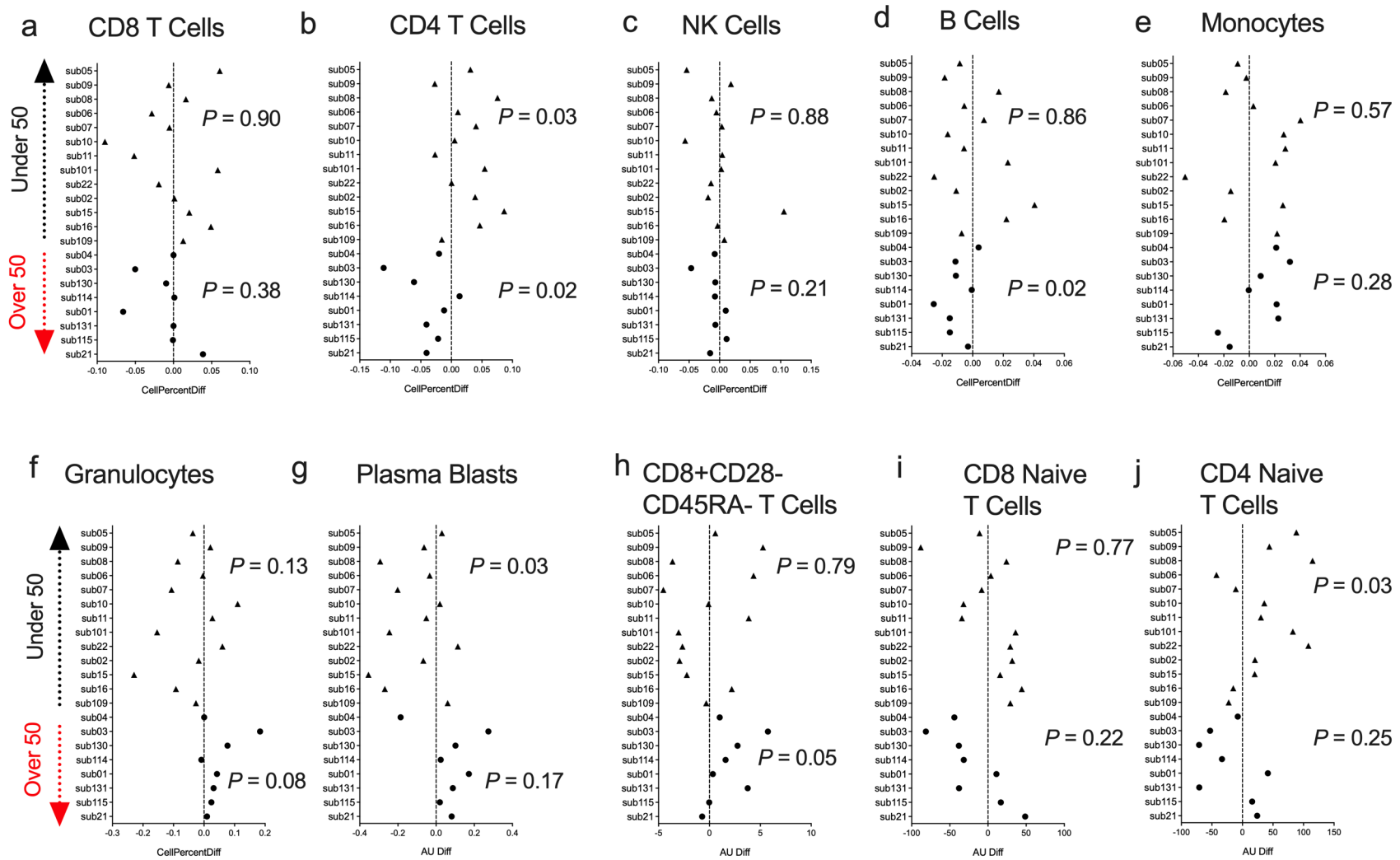
663

664

665

666

667 **FIGURE 2 DNA methylation inferred blood immune cell type composition following COVID-19 exposure.**

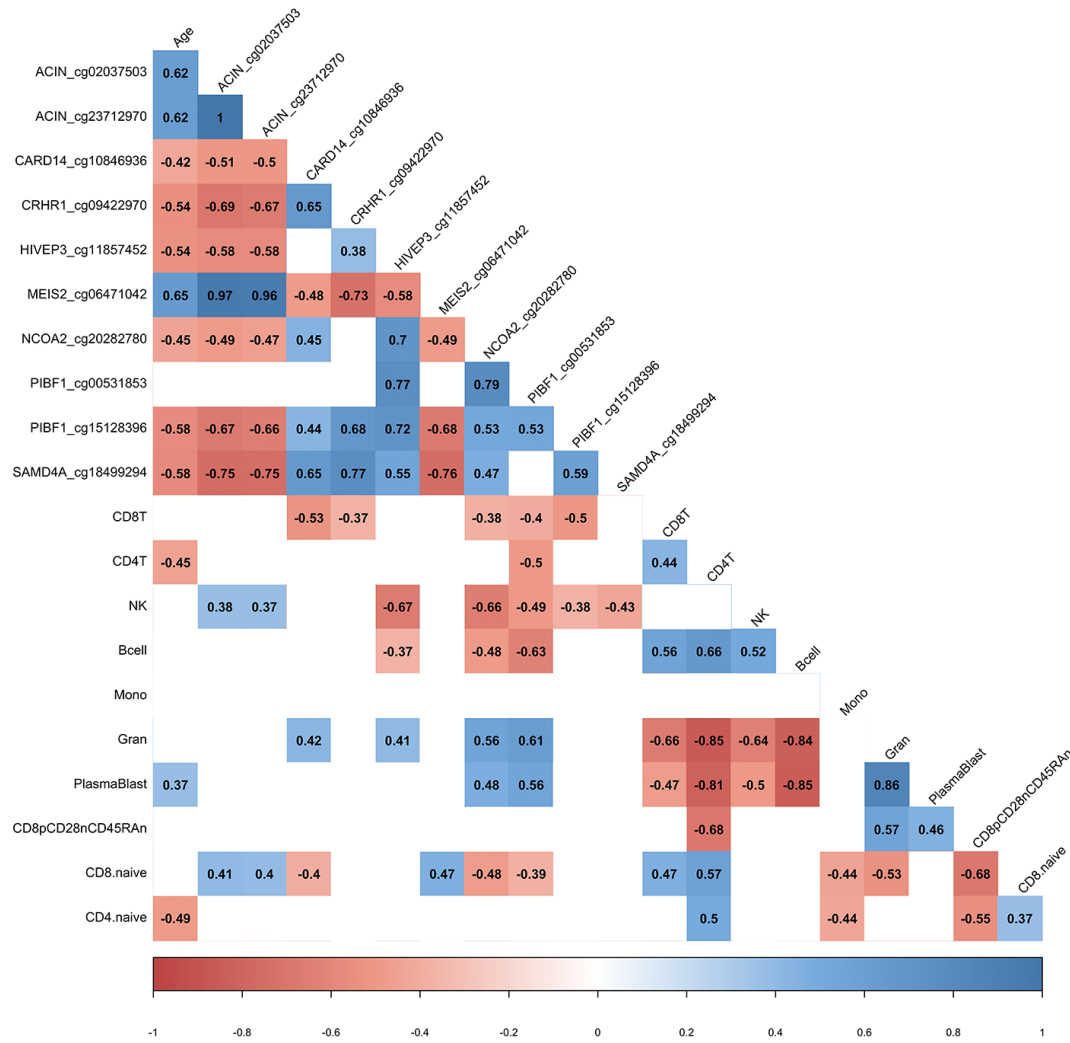


668

669

670

671 **Figure 3. DML associated with COVID-19 relate to immune cell type composition.**



672

673

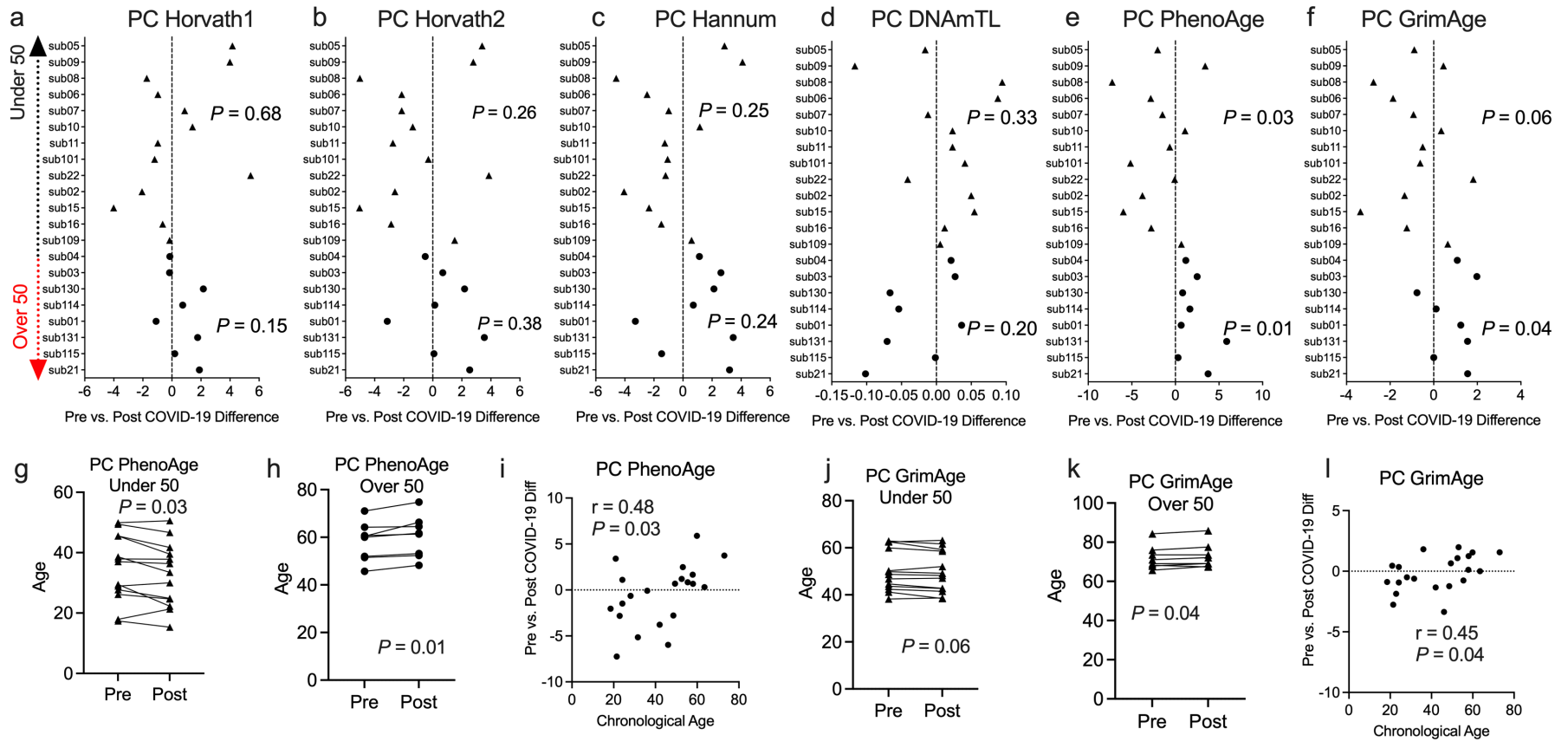
674

675

676

677

Figure 4. Divergence in principal component-based DNAmPhenoAge and GrimAge mortality risk increased based on age related to COVID-19.



678

679

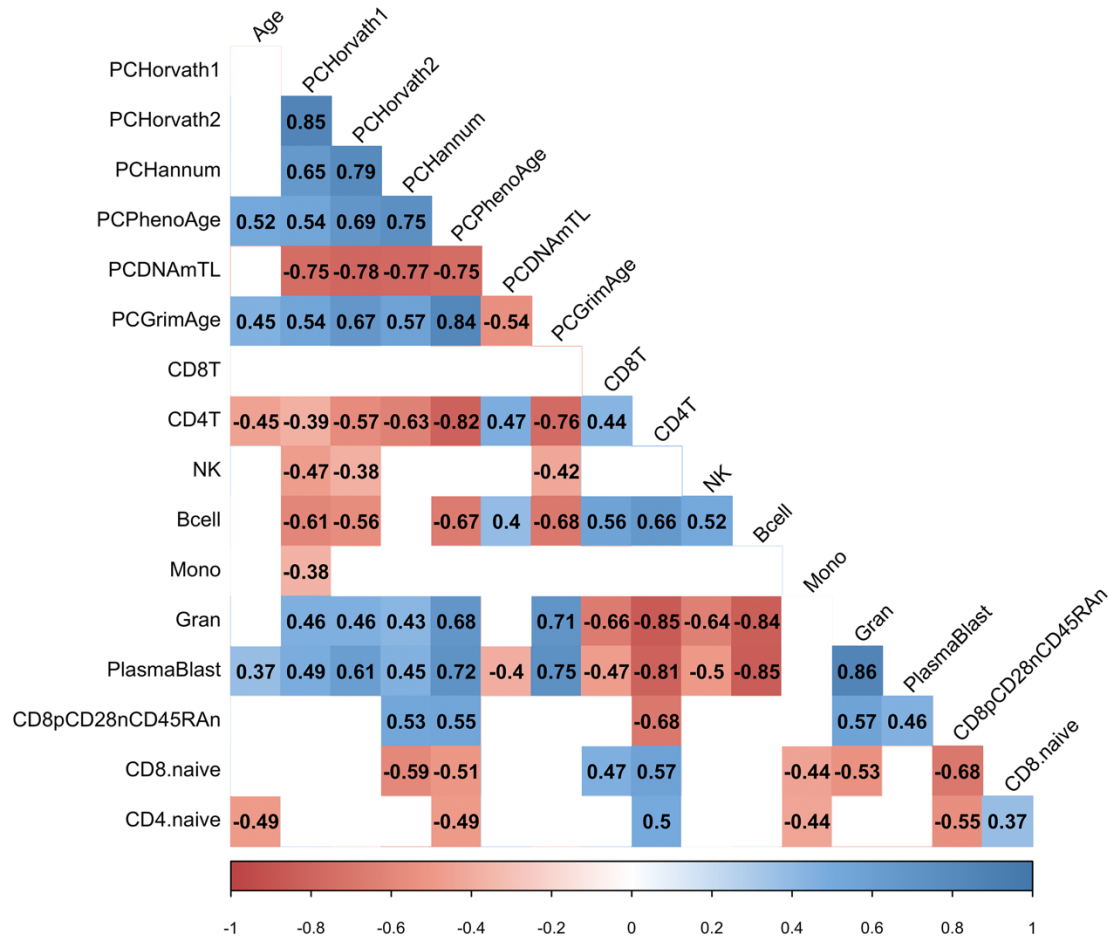
680

681

682

683

684 **Figure 5. COVID-19 related epigenetic clock changes associate with immune cell type changes.**



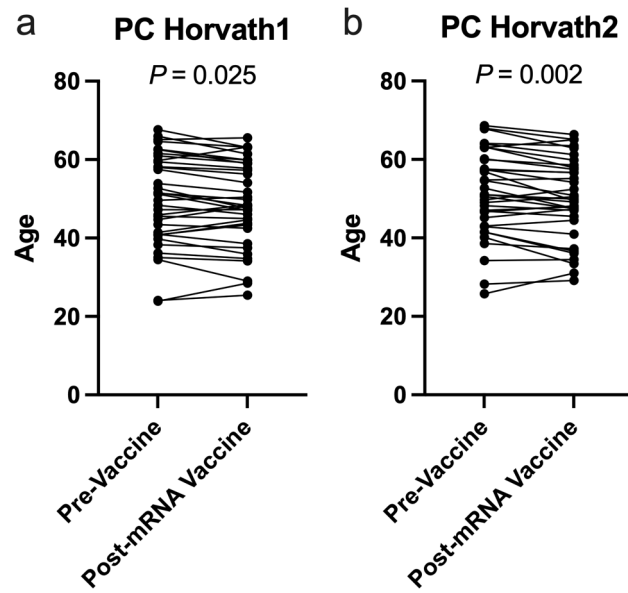
685

686

687

688

689 **Figure 6. mRNA COVID-19 vaccination decreases PCHorvath1 and PCHorvath2 epigenetic age.**



690

691

692

693

694

695

696

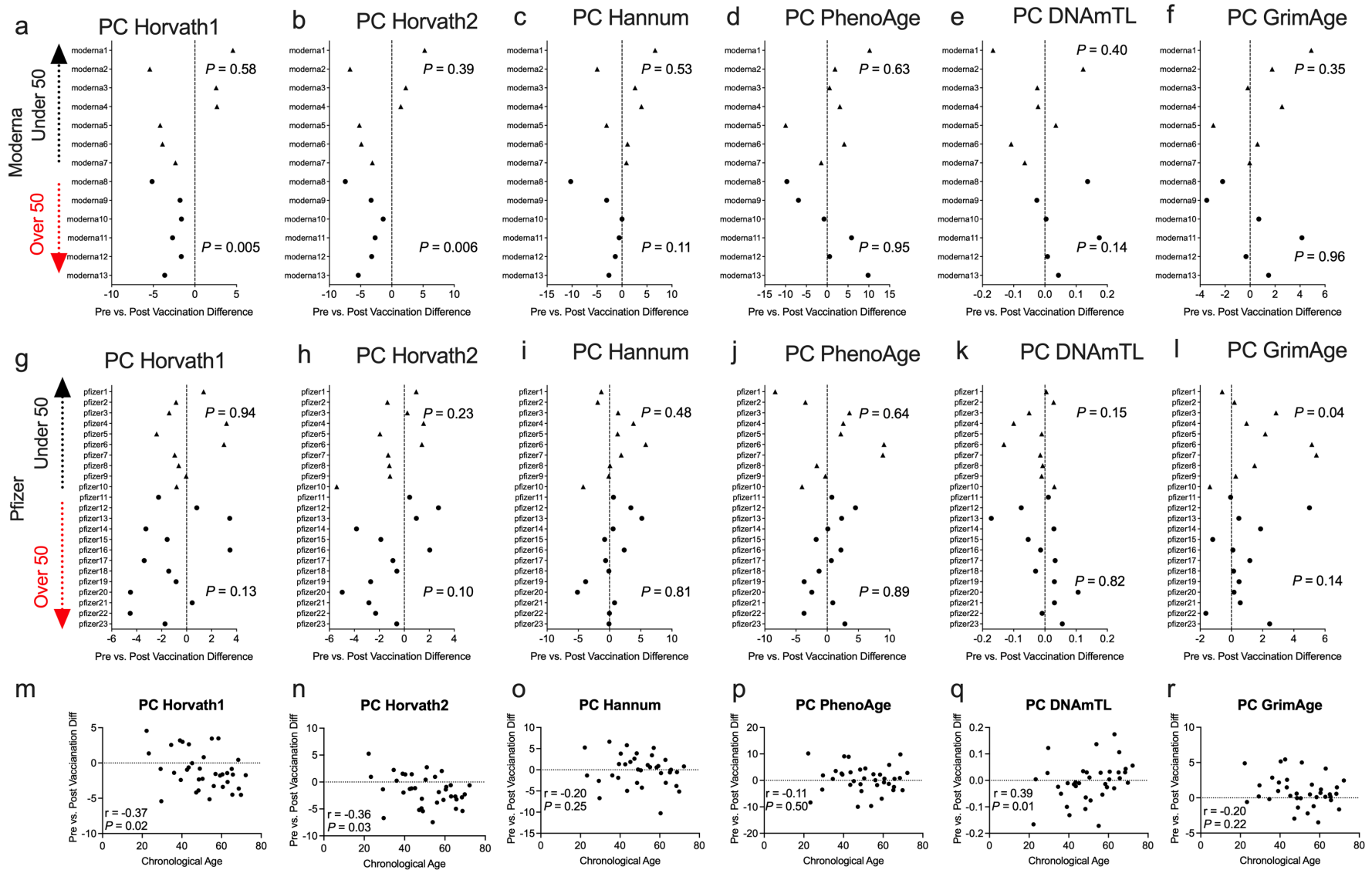
697

698

699

700

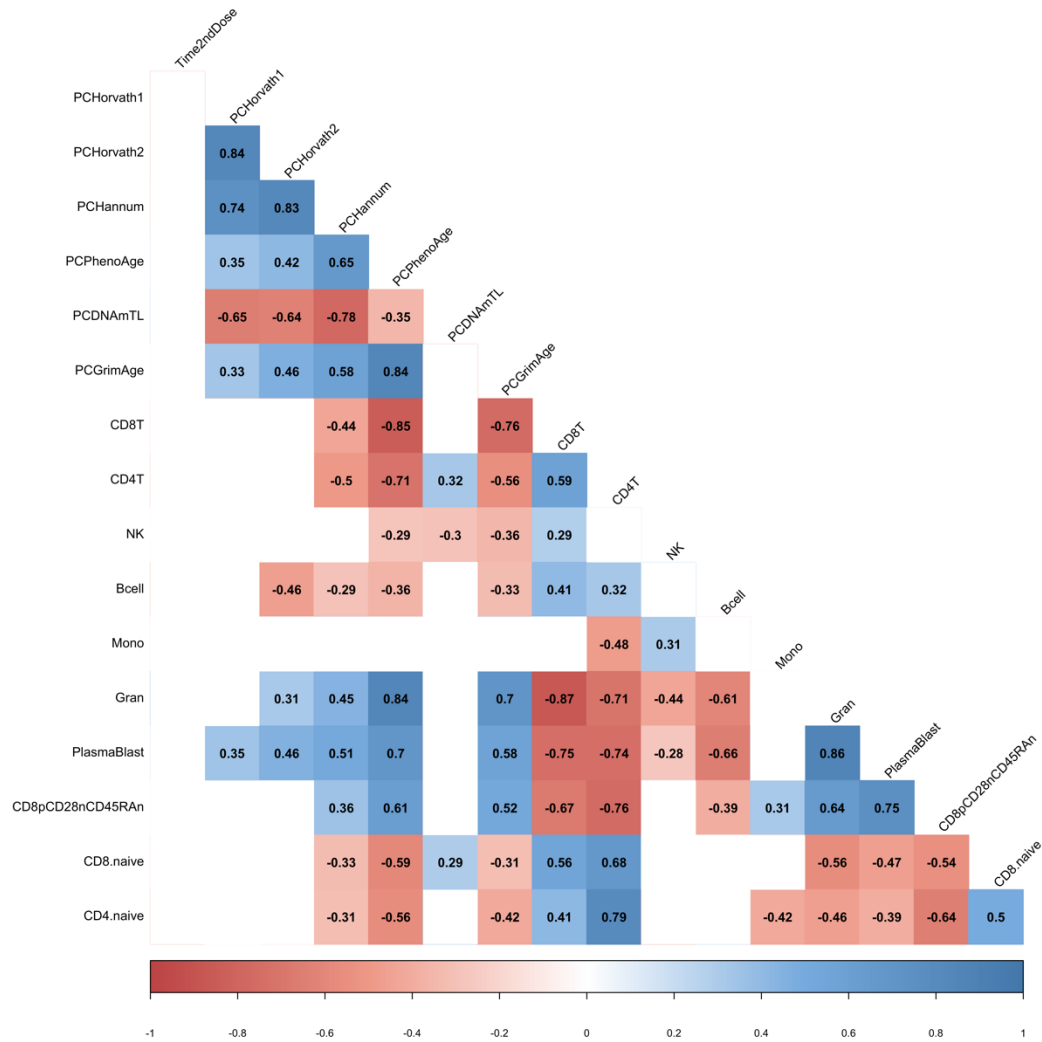
Figure 7. Moderna mRNA COVID-19 vaccination decreases principal component-based epigenetic age in individuals over 50.



701

702

703 **Figure 8. mRNA vaccine-related epigenetic clock changes associate with immune cell type changes.**



704

705

706

707

708 **7 Author Contributions**

709 MJC, LNC, RS conceived of and designed the study. MJC, APS, ATH wrote the manuscript. FC, IR,
710 CA, HW, TM, VD performed recruitment, data collection, analyses, and DNA methylation
711 experiments. MEL and ATH provided PC-Clocks algorithm. MS performed *in vitro* SARS-CoV-2
712 experiments.

713 **8 Funding**

714 NIH NHLBI K01HL140271-04, R01AG063846-02 (Corley/Ndhlovu). Thomas P. Detre Fellowship
715 Award in Translational Neuroscience Research from Yale University, Medical Informatics
716 Fellowship Program at the West Haven, CT Veterans Healthcare Administration (Higgins-Chen).
717 NIH NIA R00AG052604-04S1 (Levine).

718

719 **9 Acknowledgments**

720 We gratefully acknowledge the study participants and their physicians who made this work possible.

721

722

723

724

725

726

727

728

729

730

731

732

733

734

735

736 **10 References**

737

738 Atmar, R. L., Lyke, K. E., Deming, M. E., Jackson, L. A., Branche, A. R., El Sahly, H. M., et al.
739 (2021). Heterologous SARS-CoV-2 Booster Vaccinations - Preliminary Report. *medRxiv*.
740 doi:10.1101/2021.10.10.21264827.

741 Baden, L. R., El Sahly, H. M., Essink, B., Kotloff, K., Frey, S., Novak, R., et al. (2021). Efficacy and
742 Safety of the mRNA-1273 SARS-CoV-2 Vaccine. *N. Engl. J. Med.* 384, 403–416.

743 Balnis, J., Madrid, A., Hogan, K. J., Drake, L. A., Chieng, H. C., Tiwari, A., et al. (2021). Blood
744 DNA methylation and COVID-19 outcomes. *Clin. Epigenetics* 13, 118.

745 Belsky, D. W., Caspi, A., Arseneault, L., Baccarelli, A., Corcoran, D. L., Gao, X., et al. (2020).
746 Quantification of the pace of biological aging in humans through a blood test, the
747 DunedinPoAm DNA methylation algorithm. *Elife* 9. doi:10.7554/eLife.54870.

748 Belsky, D. W., Caspi, A., Corcoran, D. L., Sugden, K., Poulton, R., Arseneault, L., et al. (2021).
749 Quantification of the pace of biological aging in humans through a blood test: the
750 DunedinPACE DNA methylation algorithm. *bioRxiv*. doi:10.1101/2021.08.30.21262858.

751 Belsky, D. W., Caspi, A., Houts, R., Cohen, H. J., Corcoran, D. L., Danese, A., et al. (2015).
752 Quantification of biological aging in young adults. *Proc. Natl. Acad. Sci. U. S. A.* 112, E4104-
753 10.

754 Bernardes, J. P., Mishra, N., Tran, F., Bahmer, T., Best, L., Blase, J. I., et al. (2020). Longitudinal
755 Multi-omics Analyses Identify Responses of Megakaryocytes, Erythroid Cells, and
756 Plasmablasts as Hallmarks of Severe COVID-19. *Immunity* 53, 1296-1314.e9.

757 Bertin, J., Wang, L., Guo, Y., Jacobson, M. D., Poyet, J.-L., Srinivasula, S. M., et al. (2001).
758 CARD11 and CARD14 Are Novel Caspase Recruitment Domain (CARD)/Membrane-
759 associated Guanylate Kinase (MAGUK) Family Members that Interact with BCL10 and
760 Activate NF- κ B*. *J. Biol. Chem.* 276, 11877–11882.

761 Blanco-Melo, D., Nilsson-Payant, B. E., Liu, W.-C., Uhl, S., Hoagland, D., Møller, R., et al. (2020).
762 Imbalanced Host Response to SARS-CoV-2 Drives Development of COVID-19. *Cell* 181,
763 1036-1045.e9.

764 Borobia, A. M., Carcas, A. J., Pérez-Olmeda, M., Castaño, L., Bertran, M. J., García-Pérez, J., et al.
765 (2021). Immunogenicity and reactogenicity of BNT162b2 booster in ChAdOx1-S-primed
766 participants (CombiVacS): a multicentre, open-label, randomised, controlled, phase 2 trial.
767 *Lancet* 398, 121–130.

768 Bose, M., Wu, C., Pankow, J. S., Demerath, E. W., Bressler, J., Fornage, M., et al. (2014). Evaluation
769 of microarray-based DNA methylation measurement using technical replicates: the
770 Atherosclerosis Risk In Communities (ARIC) Study. *BMC Bioinformatics* 15, 312.

771 Boulias, K., Lieberman, J., and Greer, E. L. (2016). An Epigenetic Clock Measures Accelerated
772 Aging in Treated HIV Infection. *Mol. Cell* 62, 153–155.

- 773 Breeze, C. E., Reynolds, A. P., van Dongen, J., Dunham, I., Lazar, J., Neph, S., et al. (2019).
774 eFORGE v2.0: updated analysis of cell type-specific signal in epigenomic data.
775 *Bioinformatics* 35, 4767–4769.
- 776 Castro de Moura, M., Davalos, V., Planas-Serra, L., Alvarez-Errico, D., Arribas, C., Ruiz, M., et al.
777 (2021). Epigenome-wide association study of COVID-19 severity with respiratory failure.
778 *EBioMedicine* 66, 103339.
- 779 Chen, R., Xia, L., Tu, K., Duan, M., Kukurba, K., Li-Pook-Than, J., et al. (2018). Longitudinal
780 personal DNA methylome dynamics in a human with a chronic condition. *Nat. Med.*
781 doi:10.1038/s41591-018-0237-x.
- 782 Collier, D. A., Ferreira, I. A. T. M., Kotagiri, P., Datir, R. P., Lim, E. Y., Touizer, E., et al. (2021).
783 Age-related immune response heterogeneity to SARS-CoV-2 vaccine BNT162b2. *Nature*
784 596, 417–422.
- 785 Corley, M. J., Pang, A. P. S., Dody, K., Mudd, P. A., Patterson, B. K., Seethamraju, H., et al. (2021).
786 Genome-wide DNA methylation profiling of peripheral blood reveals an epigenetic signature
787 associated with severe COVID-19. *J. Leukoc. Biol.* doi:10.1002/JLB.5HI0720-466R.
- 788 Doria-Rose, N., Suthar, M. S., Makowski, M., O’Connell, S., McDermott, A. B., Flach, B., et al.
789 (2021). Antibody Persistence through 6 Months after the Second Dose of mRNA-1273
790 Vaccine for Covid-19. *N. Engl. J. Med.* 384, 2259–2261.
- 791 Epel, E. S. (2020). The geroscience agenda: Toxic stress, hormetic stress, and the rate of aging.
792 *Ageing Res. Rev.* 63, 101167.
- 793 Franzen, J., Nüchtern, S., Tharmapalan, V., Vieri, M., Nikolić, M., Han, Y., et al. (2021). Epigenetic
794 Clocks Are Not Accelerated in COVID-19 Patients. *Int. J. Mol. Sci.* 22.
795 doi:10.3390/ijms22179306.
- 796 Gensous, N., Franceschi, C., Blomberg, B. B., Pirazzini, C., Ravaioli, F., Gentilini, D., et al. (2018).
797 Responders and non-responders to influenza vaccination: A DNA methylation approach on
798 blood cells. *Exp. Gerontol.* 105, 94–100.
- 799 Gómez-Díaz, E., Jordà, M., Peinado, M. A., and Rivero, A. (2012). Epigenetics of host-pathogen
800 interactions: the road ahead and the road behind. *PLoS Pathog.* 8, e1003007.
- 801 Griffin, P. T., Kane, A. E., Trapp, A., Li, J., McNamara, M. S., Meer, M. V., et al. (2021). Ultra-
802 cheap and scalable epigenetic age predictions with TIME-Seq. *bioRxiv*, 2021.10.25.465725.
803 doi:10.1101/2021.10.25.465725.
- 804 Hannum, G., Guinney, J., Zhao, L., Zhang, L., Hughes, G., Sada, S., et al. (2013). Genome-wide
805 methylation profiles reveal quantitative views of human aging rates. *Mol. Cell* 49, 359–367.
- 806 Higgins-Chen, A. T., Thrush, K. L., and Levine, M. E. (2021a). Aging biomarkers and the brain.
807 *Semin. Cell Dev. Biol.* 116, 180–193.
- 808 Higgins-Chen, A. T., Thrush, K. L., Wang, Y., Kuo, P.-L., Wang, M., Minter, C. J., et al. (2021b).
809 A computational solution for bolstering reliability of epigenetic clocks: Implications for

- 810 clinical trials and longitudinal tracking. *bioRxiv*, 2021.04.16.440205.
811 doi:10.1101/2021.04.16.440205.
- 812 Hillary, R. F., Stevenson, A. J., Cox, S. R., McCartney, D. L., Harris, S. E., Seeboth, A., et al. (2021).
813 An epigenetic predictor of death captures multi-modal measures of brain health. *Mol.*
814 *Psychiatry* 26, 3806–3816.
- 815 Hillary, R. F., Stevenson, A. J., McCartney, D. L., Campbell, A., Walker, R. M., Howard, D. M., et
816 al. (2020). Epigenetic measures of ageing predict the prevalence and incidence of leading
817 causes of death and disease burden. *Clin. Epigenetics* 12, 115.
- 818 Horvath, S. (2013). DNA methylation age of human tissues and cell types. *Genome Biol.* 14, R115.
- 819 Horvath, S., and Levine, A. J. (2015). HIV-1 Infection Accelerates Age According to the Epigenetic
820 Clock. *J. Infect. Dis.* 212, 1563–1573.
- 821 Horvath, S., Oshima, J., Martin, G. M., Lu, A. T., Quach, A., Cohen, H., et al. (2018). Epigenetic
822 clock for skin and blood cells applied to Hutchinson Gilford Progeria Syndrome and ex vivo
823 studies. *Aging* 10, 1758–1775.
- 824 Horvath, S., and Raj, K. (2018). DNA methylation-based biomarkers and the epigenetic clock theory
825 of ageing. *Nat. Rev. Genet.* 19, 371–384.
- 826 Houseman, E. A., Accomando, W. P., Koestler, D. C., Christensen, B. C., Marsit, C. J., Nelson, H.
827 H., et al. (2012). DNA methylation arrays as surrogate measures of cell mixture distribution.
828 *BMC Bioinformatics* 13, 86.
- 829 Huoman, J., Sayyab, S., Apostolou, E., Karlsson, L., Porcile, L., Rizwan, M., et al. (2021). Mild
830 SARS-CoV-2 infection modifies DNA methylation of peripheral blood mononuclear cells
831 from COVID-19 convalescents. *bioRxiv*. doi:10.1101/2021.07.05.21260014.
- 832 Kuleshov, M. V., Clarke, D. J. B., Kropiwnicki, E., Jagodnik, K. M., Bartal, A., Evangelista, J. E., et
833 al. (2020). The COVID-19 Gene and Drug Set Library. *Res Sq*. doi:10.21203/rs.3.rs-
834 28582/v1.
- 835 Kuleshov, M. V., Jones, M. R., Rouillard, A. D., Fernandez, N. F., Duan, Q., Wang, Z., et al. (2016).
836 Enrichr: a comprehensive gene set enrichment analysis web server 2016 update. *Nucleic*
837 *Acids Res.* 44, W90-7.
- 838 Kuo, C.-L., Pilling, L. C., Atkins, J. C., Masoli, J., Delgado, J., Tignanelli, C., et al. (2020). COVID-
839 19 severity is predicted by earlier evidence of accelerated aging. *medRxiv*.
840 doi:10.1101/2020.07.10.20147777.
- 841 Levin, E. G., Lustig, Y., Cohen, C., Fluss, R., Indenbaum, V., Amit, S., et al. (2021). Waning
842 Immune Humoral Response to BNT162b2 Covid-19 Vaccine over 6 Months. *N. Engl. J. Med.*
843 doi:10.1056/NEJMoa2114583.
- 844 Levine, M. E., Lu, A. T., Quach, A., Chen, B. H., Assimes, T. L., Bandinelli, S., et al. (2018). An
845 epigenetic biomarker of aging for lifespan and healthspan. *Aging* 10, 573–591.

- 846 Liu, Z., Leung, D., Thrush, K., Zhao, W., Ratliff, S., Tanaka, T., et al. (2020). Underlying features of
847 epigenetic aging clocks in vivo and in vitro. *Aging Cell* 19, e13229.
- 848 Logue, M. W., Smith, A. K., Wolf, E. J., Maniates, H., Stone, A., Schichman, S. A., et al. (2017).
849 The correlation of methylation levels measured using Illumina 450K and EPIC BeadChips in
850 blood samples. *Epigenomics* 9, 1363–1371.
- 851 Lu, A. T., Quach, A., Wilson, J. G., Reiner, A. P., Aviv, A., Raj, K., et al. (2019). DNA methylation
852 GrimAge strongly predicts lifespan and healthspan. *Aging* 11, 303–327.
- 853 Mongelli, A., Barbi, V., Gottardi Zamperla, M., Atlante, S., Forleo, L., Nesta, M., et al. (2021a).
854 Evidence for Biological Age Acceleration and Telomere Shortening in COVID-19 Survivors.
855 *Int. J. Mol. Sci.* 22. doi:10.3390/ijms22116151.
- 856 Mongelli, A., Barbi, V., Zamperla, M. G., Atlante, S., Forleo, L., Nesta, M., et al. (2021b). Evidence
857 for biological age acceleration and telomere shortening in covid-19 survivors. *bioRxiv*.
858 doi:10.1101/2021.04.23.21255973.
- 859 Morales-Nebreda, L., McLafferty, F. S., and Singer, B. D. (2019). DNA methylation as a
860 transcriptional regulator of the immune system. *Transl. Res.* 204, 1–18.
- 861 Mueller, A. L., McNamara, M. S., and Sinclair, D. A. (2020). Why does COVID-19
862 disproportionately affect older people? *Aging* 12, 9959–9981.
- 863 Najarro, K., Nguyen, H., Chen, G., Xu, M., Alcorta, S., Yao, X., et al. (2015). Telomere Length as an
864 Indicator of the Robustness of B- and T-Cell Response to Influenza in Older Adults. *J. Infect.*
865 *Dis.* 212, 1261–1269.
- 866 Nordström, P., Ballin, M., and Nordström, A. (2021). Effectiveness of heterologous ChAdOx1
867 nCoV-19 and mRNA prime-boost vaccination against symptomatic Covid-19 infection in
868 Sweden: A nationwide cohort study. *Lancet Reg Health Eur*, 100249.
- 869 Oblak, L., van der Zaag, J., Higgins-Chen, A. T., Levine, M. E., and Boks, M. P. (2021). A
870 systematic review of biological, social and environmental factors associated with epigenetic
871 clock acceleration. *Ageing Res. Rev.* 69, 101348.
- 872 Pidsley, R., Zotenko, E., Peters, T. J., Lawrence, M. G., Risbridger, G. P., Molloy, P., et al. (2016).
873 Critical evaluation of the Illumina MethylationEPIC BeadChip microarray for whole-genome
874 DNA methylation profiling. *Genome Biol.* 17, 208.
- 875 Plassmeyer, M., Alpan, O., Corley, M. J., Premeaux, T. A., Lillard, K., Coatney, P., et al. (2021).
876 Caspases and therapeutic potential of caspase inhibitors in moderate-severe SARS CoV2
877 infection and long COVID. *Allergy*. doi:10.1111/all.14907.
- 878 Polack, F. P., Thomas, S. J., Kitchin, N., Absalon, J., Gurtman, A., Lockhart, S., et al. (2020). Safety
879 and Efficacy of the BNT162b2 mRNA Covid-19 Vaccine. *N. Engl. J. Med.* 383, 2603–2615.
- 880 Pozzetto, B., Legros, V., Djebali, S., Barateau, V., Guibert, N., Villard, M., et al. (2021).
881 Immunogenicity and efficacy of heterologous ChadOx1/BNT162b2 vaccination. *Nature*.
882 doi:10.1038/s41586-021-04120-y.

- 883 Reiterer, M., Rajan, M., Gómez-Banoy, N., Lau, J. D., Gomez-Escobar, L. G., Ma, L., et al. (2021).
884 Hyperglycemia in acute COVID-19 is characterized by insulin resistance and adipose tissue
885 infectivity by SARS-CoV-2. *Cell Metab.* 33, 2174-2188.e5.
- 886 Rendeiro, A. F., Ravichandran, H., Bram, Y., Chandar, V., Kim, J., Meydan, C., et al. (2021). The
887 spatial landscape of lung pathology during COVID-19 progression. *Nature*.
888 doi:10.1038/s41586-021-03475-6.
- 889 Sahara, S., Aoto, M., Eguchi, Y., Imamoto, N., Yoneda, Y., and Tsujimoto, Y. (1999). Acinus is a
890 caspase-3-activated protein required for apoptotic chromatin condensation. *Nature* 401, 168–
891 173.
- 892 Schäfer, A., and Baric, R. S. (2017). Epigenetic Landscape during Coronavirus Infection. *Pathogens*
893 6. doi:10.3390/pathogens6010008.
- 894 Schmidt, T., Klemis, V., Schub, D., Schneitler, S., Reichert, M. C., Wilkens, H., et al. (2021).
895 Cellular immunity predominates over humoral immunity after homologous and heterologous
896 mRNA and vector-based COVID-19 vaccine regimens in solid organ transplant recipients.
897 *Am. J. Transplant.* doi:10.1111/ajt.16818.
- 898 Shaw, R. H., Stuart, A., Greenland, M., Liu, X., Nguyen Van-Tam, J. S., Snape, M. D., et al. (2021).
899 Heterologous prime-boost COVID-19 vaccination: initial reactogenicity data. *Lancet* 397,
900 2043–2046.
- 901 Soiza, R. L., Scicluna, C., and Thomson, E. C. (2021). Efficacy and safety of COVID-19 vaccines in
902 older people. *Age Ageing* 50, 279–283.
- 903 Sugden, K., Hannon, E. J., Arseneault, L., Belsky, D. W., Corcoran, D. L., Fisher, H. L., et al.
904 (2020). Patterns of Reliability: Assessing the Reproducibility and Integrity of DNA
905 Methylation Measurement. *Patterns (N Y)* 1. doi:10.1016/j.patter.2020.100014.
- 906 Tartof, S. Y., Slezak, J. M., Fischer, H., Hong, V., Ackerson, B. K., Ranasinghe, O. N., et al. (2021).
907 Effectiveness of mRNA BNT162b2 COVID-19 vaccine up to 6 months in a large integrated
908 health system in the USA: a retrospective cohort study. *Lancet*. doi:10.1016/S0140-
909 6736(21)02183-8.
- 910 Tian, Y., Morris, T. J., Webster, A. P., Yang, Z., Beck, S., Feber, A., et al. (2017). ChAMP: updated
911 methylation analysis pipeline for Illumina BeadChips. *Bioinformatics* 33, 3982–3984.
- 912 Turner, J. S., O’Halloran, J. A., Kalaidina, E., Kim, W., Schmitz, A. J., Zhou, J. Q., et al. (2021).
913 SARS-CoV-2 mRNA vaccines induce persistent human germinal centre responses. *Nature*
914 596, 109–113.
- 915 Wilk, A. J., Rustagi, A., Zhao, N. Q., Roque, J., Martínez-Colón, G. J., McKechnie, J. L., et al.
916 (2020). A single-cell atlas of the peripheral immune response in patients with severe COVID-
917 19. *Nat. Med.* 26, 1070–1076.
- 918 Wimmers, F., Donato, M., Kuo, A., Ashuach, T., Gupta, S., Li, C., et al. (2021). The single-cell
919 epigenomic and transcriptional landscape of immunity to influenza vaccination. *Cell* 184,
920 3915-3935.e21.

921 Yang, Z., Wong, A., Kuh, D., Paul, D. S., Rakyan, V. K., Leslie, R. D., et al. (2016). Correlation of
922 an epigenetic mitotic clock with cancer risk. *Genome Biol.* 17, 205.

923 Yates, K. B., Tonnerre, P., Martin, G. E., Gerdemann, U., Al Abosy, R., Comstock, D. E., et al.
924 (2021). Epigenetic scars of CD8+ T cell exhaustion persist after cure of chronic infection in
925 humans. *Nat. Immunol.* 22, 1020–1029.

926 Zheng, S. C., Breeze, C. E., Beck, S., Dong, D., Zhu, T., Ma, L., et al. (2019). EpiDISH web server:
927 Epigenetic Dissection of Intra-Sample-Heterogeneity with online GUI. *Bioinformatics.*
928 doi:10.1093/bioinformatics/btz833.

929 Zhou, S., Zhang, J., Xu, J., Zhang, F., Li, P., He, Y., et al. (2021). An epigenome-wide DNA
930 methylation study of patients with COVID-19. *Ann. Hum. Genet.* doi:10.1111/ahg.12440.

931 Zhou, W., Triche, T. J., Jr, Laird, P. W., and Shen, H. (2018). SeSAME: reducing artifactual
932 detection of DNA methylation by Infinium BeadChips in genomic deletions. *Nucleic Acids*
933 *Res.* 46, e123.

934

935

936

937

938

939

940

941

942

943

944

945

946

947

948

949

950

951

952

953

954

955

956

957 **12 Data Availability Statement**

958 The datasets generated for this study can be found in the NIH GEO database.

959 GEO Submission (Pending)

960